Topology Optimization of Electric Motor Installation

Methodology for Preliminary Design With Consideration to Crash Loads

Master's thesis in Applied Mechanics

Henrik Helmfrid
Joakim Larsson

DEPARTMENT OF INDUSTRIAL AND MATERIALS SCIENCE
CHALMERS UNIVERSITY OF TECHNOLOGY
Gothenburg, Sweden 2021
www.chalmers.se

Master's thesis 2021

Topology Optimization of Electric Motor Installation

Methodology for Preliminary Design With Consideration to Crash Loads

HENRIK HELMFRID
JOAKIM LARSSON

CHALMERS
UNIVERSITY OF TECHNOLOGY

Department of Industrial and Materials science
Division Material and Computational Mechanics
Chalmers University of Technology
Gothenburg, Sweden 2021

Topology Optimization of Electric Motor Installation
Methodology for Preliminary Design With Consideration to Crash Loads
HENRIK HELMFRID
JOAKIM LARSSON

Supervisor: Daniel Högberg, Volvo Cars
Examiner: Magnus Ekh, Department of Industrial and Materials Science

Master's Thesis 2021
Department of Industrial and Materials Science
Division of Material and Computational Mechanics
Chalmers University of Technology
SE-412 96 Gothenburg
Telephone +46 31 772 1000

Cover: Topology optimized crossmember.

Printed by Chalmers Reproservice
Gothenburg, Sweden 2021

Topology Optimization of Electric Motor Installation
Methodology for Preliminary Design With Consideration to Crash Loads
HENRIK HELMFRID
JOAKIM LARSSON
Department of Industrial and Materials Science
Chalmers University of Technology

Abstract

Early design of a large component which is subjected to a wide range of complex loads, from loads caused by extreme driving conditions to crash loads, is no easy task. In the highly competitive automotive industry, reducing weight while retaining performance is a big priority. This thesis has investigated topology optimization as a tool to aid early design for an electric engine installation. Topology optimization has the potential to produce a well defined topology while simultaneously consider several load cases, design constraints and behavioural constraints.

The load cases investigated in this thesis are engine loads, road induced loads and crash loads. The crash loads have a non-linear and transient behaviour and it has been investigated whether they can be applied as linear and static loads in an early design phase. A superelement has been used to reduce computational time while still capturing the behaviour from the body in white. As the loads vary greatly in magnitude, different constraints on different load cases have been investigated.

Through a display of different trial cases a methodology has been produced. Although more validation is desirable, the results are promising, robust and efficiently generated. As well as showing where material is needed, topology optimization can also indicate where material is not needed.

Keywords: Topology optimization, Crash loads, Superelement, Electric engine installation.

Acknowledgements

This thesis would not have been possible to carry through without the help from several people, their guidance and advice have been immensely helpful and we would therefor like to thank the following people.

First of all we would like to emphasize our appreciation to our supervisor Daniel Högberg at Volvo Cars for his enthusiastic engagement in this thesis as he went beyond his call of duty assisting us and always made time to answer our questions and connecting us with relevant people.

Thanks to our examiner Magnus Ekh who has given us valuable input and reflections during the thesis.

We would also like to thank Patrik Ljungbäck who has supported us with several key steps of this thesis. His assistance within topology optimization and setting up a superelement have invaluable. Further, we would also like to send our appreciation to Joakim Lindholm and Emil Norberg at Altair for their valuable feedback during the thesis and assisting us with their advanced software. We would also like to thank the crash department for providing us with load data from their simulations.

Lastly, we would like to thank our depertment Electric Driveline Dimensioning and especially Jesper Larsson, Henrik Åkesson and Anton Wahnström in the Mounts CAE team for their assistance and friendliness during this spring, it has been a joy to be a part of the group.

Henrik Helmfrid and Joakim Larsson, Gothenburg, May 2021

Nomenclature

Abbreviations

BIW	Body In White
CAD	Computer Aided Design
CAE	Computer Aided Engineering
CPU	Central Processing Unit
DOF	Degrees Of Freedom
FE	Finite Element
FEM	Finite Element Method
HPDC	High Pressure Die Casting
MFD	Method of Feasible Directions
RBE2	Rigid Body Element 2, infinite stiffness
RBE3	Rigid Body Element 3, no stiffness, distributing
SIMP	Solid Isotropic Material with Penalization
VCC	Volvo Car Corporation

Symbols

c	Compliance
E	Young's modulus
E^0	Young's modulus of unchanged element
f	Objective function
$\boldsymbol{f}$	Load vector
g	State function
$\hat{H}$	Weight factor for sensitivity filter
$\boldsymbol{K}$	Stiffness matrix
S	Compliance index
$\boldsymbol{u}$	Displacement vector
w	Weight factor for the objective function
W	Weight factor for compliance
$\boldsymbol{x}$	Design variable
$\boldsymbol{y}$	State variable
ν	Poisson's ratio
σ_u	Ultimate tensile strength
σ_y	Yield strength
Ω	Design space
Ω_{mat}	Material layout after optimization
ρ	Density
λ	Eigenvalue of stiffness matrix
ε_f	Rupture strain

Contents

List of Figures

List of Tables

1

Introduction

This chapter presents the necessary information to get the reader a thorough understanding of the background to the master thesis work with aims and delimitations.

1.1 Background

The department Powertrain Suspension at Volvo Cars works with the installation of the engine and focuses on damping out the vibrations and noise from the engine while ensuring a smooth ride and responsive handling. Under extreme driving conditions high loads can be exerted on the brackets holding the engine. The brackets are attached to the transmission, engine and the car body side with screw joints varying from M10-M12. The surrounding components and their position are shown in figure 1.1.

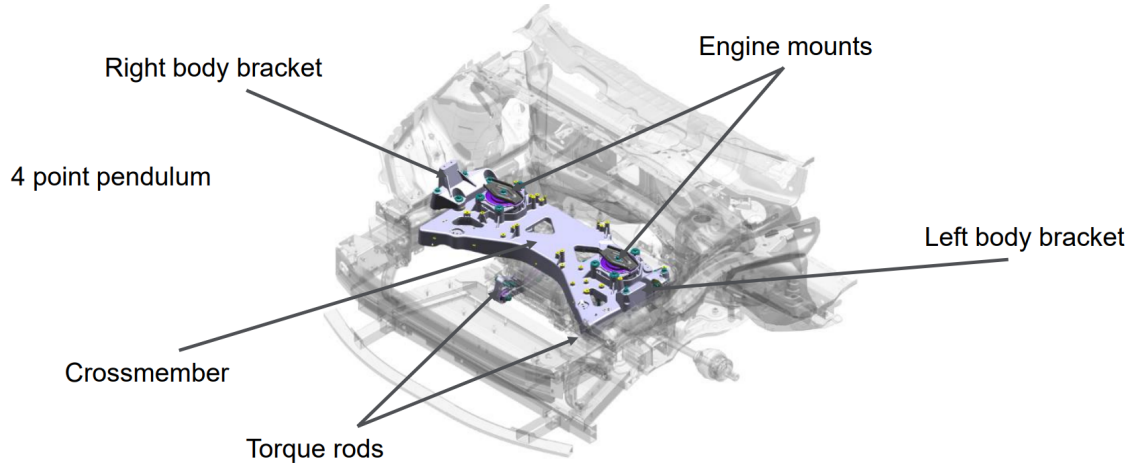

Figure 1.1: An overview of the different components in the system.

Currently, Volvo Cars uses a crossmember as a mount for some of their E-machines (electric engine + gearbox), which in addition to securing the engine also have important functions in some crash scenarios. In addition, because of the size and

rigidity of the crossmember, many components are directly attached to it. To design a component to optimally sustain such complex loads is a challenge.

Topology optimization is a method that can produce the optimal material layout for given loads and boundary conditions within a design space. For complex loadings, the early design stage of structures is often predominated by engineering experience. Thus it could be time consuming and difficult to produce a well functioning early design, while it is also difficult to divert from an early design at later stages when more information is available. Using topology optimization in the early stages of design could give the designers more information early in the development phase, when the freedom in the problem is largest.

In the highly competitive automotive industry, it is of utmost importance to produce lightweight components to improve the performance of the car while reducing costs. Components that have not been optimized can be heavier than necessary since it is hard to directly design the best topology considering that the optimal shape can be counter intuitive. A light component will also result in a more efficient ride since less energy will be needed to power the car. Manufacturing components also have a negative impact on the climate as there is a significant carbon footprint when producing metals. Topology optimization can therefor reduce the carbon footprint of the specific component since it will contain less material.

1.2 Purpose

The purpose of this thesis is to establish a methodology for topology optimization in early design phases for a mounting crossmember in E-machine installation. The optimization shall include loads which occur during regular and extreme driving, as well as more complex loads which occur during frontal crashes. The methodology will include choices of design parameters and constraints to propose suitable guidelines when performing topology optimization.

1.3 Aims and objectives

The possibility of using topology optimization for complex loaded structures in E-machine installations will be evaluated. Various optimization methods within topology optimization will be analysed to reach a suitable approach when dealing with complex loading and structures. Load cases will primarily include the engine related loads and crash loads. The thesis will also evaluate if road induced loads are of importance when optimizing the crossmember in an early design phase.

1.4 Delimitations

This thesis will focus on the methodology of topology optimization in early design stages of a mounting crossmember. Intrinsically, the thesis will mainly consider the procedures of the optimization process. As a consequence of including crash loads,

the optimization process will be dependent on loads exerted by other components. The loads will be modeled as static linear loads, which are given by measurements from earlier crash tests and simulations. The crash loads imply permanent plastic deformation, but only linear material and FE-models will be used.

Furthermore, there will be no physical validation of the model. The project will rely to the extent that is possible on that the CAE results are trustworthy, and possible encroachments of this assumption will be discussed. Finally, the optimization will not take fatigue into account.

2

Theory

This section will briefly present theory of structural optimization and its mathematical concepts in general. Further, the subclass topology optimization and its application within commercial programs will be introduced. The majority of the theory presented here is based on [Bendsoe and Sigmund, 2013] and [Christensen and Klarbring, 2008] which the reader is encouraged to read for more information about structural and topology optimization.

2.1 Structural optimization

A structural optimization seeks the best structure for a given load case. Mathematically, it can be described as either minimizing or maximizing an objective function (f) dependent on design variable ($\boldsymbol{x}$) and state variable ($\boldsymbol{y}$). The objective function is commonly the volume or the compliance, but it can be a wide range of different objectives. The objective function returns a value which represents the goodness of the design, which is often set up as to minimize its value. The design variable describes the design as a function or vector which can be altered during the optimization. Commonly it is the geometry of the design but can also be the choice of material. Finally, the state variable is the response of the design. In other words, it is chosen from some kind of requirement specified by the designer and could be for example displacement, stress, strain or force. The state variable thus depend on the design variable as $\boldsymbol{y}(\boldsymbol{x})$. The problem then becomes

$$\begin{cases} \text{minimize } f(\boldsymbol{x}, \boldsymbol{y}(\boldsymbol{x})) \text{ with respect to } \boldsymbol{x} \text{ and } \boldsymbol{y}(\boldsymbol{x}) \\ \\ \text{subject to } \begin{cases} \text{behavioral constraints on } \boldsymbol{y} \\ \text{design constraints on } \boldsymbol{x} \\ \text{equilibrium constraint} \end{cases} \end{cases} \tag{2.1}$$

It is possible to have more than one object function, called multiple criteria optimization problem. This can be written as

$$\text{minimize } (f_1(\boldsymbol{x}, \boldsymbol{y}), f_2(\boldsymbol{x}, \boldsymbol{y}), \ldots, f_l(\boldsymbol{x}, \boldsymbol{y})) \tag{2.2}$$

where l is the number of objective functions. This implies that there is no global minimum for all f_i as the different objective functions are dependent on the same design and state variables. Therefor it is generally more suitable to use a so-called Pareto optimality. One then searches for a design in which there does not exist a design that satisfies all the objective functions better. A design $(\boldsymbol{x}^*, \boldsymbol{y}^*)$ is Pareto optimal if there is no other design $(\boldsymbol{x}, \boldsymbol{y})$ that satisfies the constraints as

$$\begin{aligned} f_i(\boldsymbol{x}, \boldsymbol{y}) &\leq f_i(\boldsymbol{x}^*, \boldsymbol{y}^*) && \text{for all } i = 1, \ldots, l \\ f_i(\boldsymbol{x}, \boldsymbol{y}) &< f_i(\boldsymbol{x}^*, \boldsymbol{y}^*) && \text{for at least one } i = \{1, \ldots, l\} \end{aligned} \tag{2.3}$$

One way to solve this is to introduce a scalar objective functions with weight factors

$$f = \sum_{i=1}^{l} w_i f_i(\boldsymbol{x}, \boldsymbol{y}) \tag{2.4}$$

where l is the total number of objective functions and the sum of the weight factors is

$$\sum_{i=1}^{l} w_i = 1 \tag{2.5}$$

Depending on how the weight factors are specified different Pareto optima might be found. Equation (2.1) references behavioral, design and equilibrium constraints. The behavioral constraint is applied to the state variable $\boldsymbol{y}$ and is usually written with a state function as $g(\boldsymbol{y})$. The state function is usually constructed such that $g(\boldsymbol{y}) \leq 0$. If, for example, the behavioral constraint is a displacement constraint, it can instead be written as $g(\boldsymbol{u}(\boldsymbol{x}))$ where $\boldsymbol{u}$ is the selected nodal displacements. For a linear FE problem, these are obtained by solving:

$$\boldsymbol{K}\boldsymbol{u}(\boldsymbol{x}) = \boldsymbol{f} \tag{2.6}$$

where $\boldsymbol{K}$ is the global stiffness matrix and $\boldsymbol{f}$ is the force vector. Thus the behavioral constraint coincides with the equilibrium constraint, which is simply equation (2.6). The design constraint is applied to the design variable $\boldsymbol{x}$ and, as the name suggests, infers constraints on the design or geometry. By structuring the state function as a combination of state and design constraints, the structural optimization problem can be stated as a nested formulation:

$$\begin{cases} \min & f(\boldsymbol{x}, \boldsymbol{u}(\boldsymbol{x})) \\ \text{such that} & g(\boldsymbol{x}, \boldsymbol{u}(\boldsymbol{x})) \leq 0 \end{cases} \tag{2.7}$$

2.2 Topology optimization

Topology optimization is the most broad type of structural optimization. Within topology optimization the material can take any form and is therefor beneficially used in the early design phases of products. The method optimizes a material layout within a defined design space based on boundary conditions, load cases and the given objective or objectives to optimize. The design space is the volume where the component is allowed transform into its optimal shape. Contrarily, the volume which is not allowed to transformed is called the non-design space. A finite element discretization of the volume is done in order to begin the optimization.

Topology optimization is an iterative scheme where the FE-problem is solved for the provided load case and material is thereafter removed or redistributed. Lastly, a convergence check is executed. The convergence is a correlation between the design of the previous iteration and the objective functions, the purpose is to see if only insignificant changes have been performed. If convergence has been fulfilled according to a defined criteria, the optimization has been completed, otherwise the iteration procedure starts over from the FE-problem.

2.2.1 Solid Isotropic Material with Penalization method

The objective is to find $\Omega_{mat} \in \Omega$ where Ω is the specified design space. The design variables $\boldsymbol{x}$ defined in section 2.1 is replaced with $\boldsymbol{\rho}$, which represents the density where ρ_e is the density of each individual element in the volume. The component's stiffness is then represented by equation 2.8. This formulations results in a discrete design value problem, also known as a 0-1 problem. E_{ijkl} is the effective stiffness tensor and can be formulated as.

$$E_{ijkl} = \boldsymbol{\rho}\, E^0_{ijkl}, \quad \boldsymbol{\rho} = \begin{cases} 1 \text{ if } \rho_e \in \Omega_{mat} \\ 0 \text{ if } \rho_e \in \Omega \backslash \Omega_{mat} \end{cases} \tag{2.8}$$

together with the volume constraint:

$$\int_\Omega \boldsymbol{\rho}\, d\Omega = \text{Vol}(\Omega_{mat}) \leq Vol(\Omega) \tag{2.9}$$

$\rho_e = 1$ indicates that an element is filled whilst $\rho_e = 0$ indicates that the element is void. E^0_{ijkl} is the stiffness tensor for the elastic material. To solve this problem with a gradient based approach, the integer variables in equation 2.8 needs to be continuous. A popular way of solving this is to implement the Solid Isotropic Material with Penalization method (SIMP). SIMP is an interpolation scheme which adopts a penalization factor, p, that penalizes elements with intermediate densities $(0 < \rho < 1)$.

$$\begin{aligned} E_{ijkl} &= \boldsymbol{\rho}^p\, E^0_{ijkl}, & p &> 1 \\ \int_\Omega \boldsymbol{\rho} d\Omega &\leq Vol(\Omega), & 0 \leq \boldsymbol{\rho} &\leq 1 \end{aligned} \tag{2.10}$$

In SIMP, choosing a penalization factor of $p > 1$ will lead to unfavorability of intermediate densities since their gain (stiffness) will not outweigh their cost (volume). The SIMP method's penalization is achieved without using an explicit penalization scheme. To achieve a correct 0-1 solution, $p \geq 3$ is generally required. Figure 2.1 depicts the effects of the SIMP-method where a higher penalization factor will result in an steeper curve. However, a higher value of p decreases the robustness of the solution.

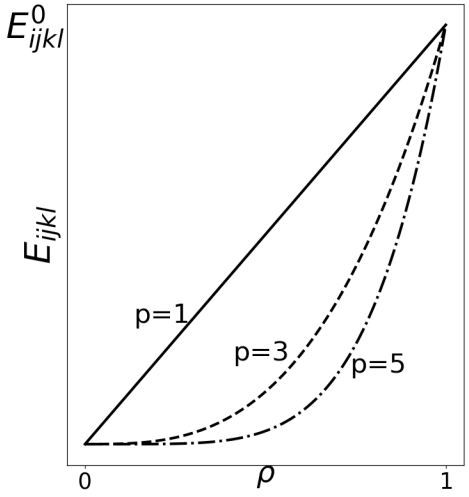

Figure 2.1: The effect of different penalization factors in relation to the stiffness tensor, E^0_{ijkl}, and the effective stiffness tensor, E_{ijkl}.

2.2.2 Compliance

When designing a load bearing component a high stiffness and low weight is often desired. To obtain this from topology optimization, one minimizes the compliance of the component. If the stiffness requirement is known, the problem can instead be to minimize weight (or volume) while having a constraint on the compliance. Mathematically the compliance c is defined as:

$$c = \boldsymbol{f}^T \boldsymbol{u} \tag{2.11}$$

where $\boldsymbol{f}$ and $\boldsymbol{u}$ are the external load and displacement vectors respectively. Decreasing the displacement at the location of the force will decrease the compliance, thus increasing the stiffness. One can think of the compliance as the inverse of the stiffness, or the work generated by external forces. The optimization problem then becomes

$$\begin{cases} \min & \boldsymbol{f}^T \boldsymbol{u} \quad (= c) \\ \text{such that} & \boldsymbol{K}(E_{ijkl})\boldsymbol{u} = \boldsymbol{f} \end{cases} \tag{2.12}$$

2.2.2.1 Weighted compliance

A way to effectively take into account multiple load cases is to minimize weighted compliance [Altair, 2021]. It is calculated as

$$C_W = \sum_i W_i c_i \tag{2.13}$$

where W_i is a weight factor for each load case and c_i is the compliance[Altair, 2021]. Introducing weight factors makes it possible to equalize load cases, as different load cases can have large variation in compliance. The optimization problem can then be defined similarly as before, but with the weighted instead of compliance:

$$\begin{cases} \min & C_W \\ \text{such that} & \boldsymbol{K}(E_{ijkl})\boldsymbol{u} = \boldsymbol{f} \end{cases} \tag{2.14}$$

2.2.3 Challenges with topology optimization

There are many challenges with topology optimization, and the designers need to keep these in mind when conducting a topology optimization. The most prevalent ones are checkerboarding, its dependence on mesh resolution and the problem of attaining a global minimum. This section will explain why these problems exist and how to avoid them.

2.2.3.1 Mesh dependency

The outcome of a topology optimization is heavily dependent on mesh resolution. A finer mesh allows for more complex structures to be generated as illustrated by figure 2.2. Generally, by introducing more holes in a structure while still retaining the same volume, its efficiency will increase. If the mesh is refined enough, microstructures can be generated which can not be assumed to be isotropic. As such there exists no single solution to a topology optimization. One method of combating the non-uniqueness of topology optimization which has proved to be highly effective is to introduce a sensitivity filter. The advantages are that it does not require much more CPU-time, and no new constraints are needed on the optimization. The design sensitivity is altered with respect to the objective function for a specific element based on the weighted average of a fixed number of neighbouring elements. It is done as

$$\widehat{\frac{\partial f}{\partial \rho_k}} = \frac{1}{\rho_k \sum_{i=1}^{N} \hat{H}_i} \sum_{i=1}^{N} \hat{H}_i \rho_i \frac{\partial f}{\partial \rho_i} \tag{2.15}$$

where $\hat{H}_i$ is the weight factor which is based on the distance to the neighbouring elements. It is written as $\hat{H}_i = r_{min} - \text{dist}(k, i)$ where $\text{dist}(k, i)$ is the distance between the center of the neighbouring element i and current element k.

(a) 800 elements. **(b)** 20000 elements.

Figure 2.2: Topology optimization of an MBB beam resulting in different optimal structures depending on number of elements used. Generated in MATLAB using 88 lines of code [Andreassen et al., 2011].

2.2.3.2 Checkerboarding

Checkerboarding is when every other element is removed, leaving a checkerboard pattern of solid and void elements, see figure 2.3. These structures can have a very high artificial stiffness, but the structures are non physical. They arise due to numerical errors in the FE formulation which overestimates the stiffness of these patterns. To avoid this phenomenon, a sensitivity filter can be implemented which acts similar as the filter described in equation (2.15). This filter makes the design sensitivity of a specific element depend on the weighted average of itself and eight neighbouring elements. Another remedy to this problem is to implement a minimum allowable member condition or higher order elements. The minimum allowable member condition essentially prohibits the optimization algorithm to create holes which are smaller than a specified value. The problem with higher order elements however is that they significantly increase the computational time. Thus if the purpose is only to avoid checkerboarding the other methods are more computationally efficient.

(a) Sensitivity filter turned on. **(b)** Sensitivity filter turned off which generates a checkerboard pattern.

Figure 2.3: Topology optimization of an MBB beam with and without sensitivity filter in MATLAB using 88 lines of code [Andreassen et al., 2011].

2.2.3.3 Large deformations

Large deformations are extremely complicated in topology optimization. Many problems can arise, for example the topology optimization can generate a structure which performs well for the given loads, but any alteration in magnitude or direction of force may cause the structure to collapse. As such, the thesis will model large transient loads (crash loads) which can produce large plastic deformation as static loads.

2.3 Optimization in OptiStruct

The topology optimization in this thesis will be accomplished by using the solver OptiStruct. The solver uses a gradient-based approach to achieve to the optimal design. Gradient-based method are mainly used since they can handle multiple constraints while being effective in terms of computational speed. A drawback is that the approach is sensitive to the initial conditions and is thus not robust. The *Method of Feasible Directions* (MFD) [Altair, 2021] is the default algorithm in OptiStruct. It is an iterative method which starts from a possible location in the design space and then searches for the next improved feasible point. Other algorithms such as Sequential quadratic programming and Dual Optimizer based on separate convex approximation are also available.

OptiStruct also uses SIMP as default (see section 2.2.1). For a solid-dominant structure, the penalization factor is set to two in the beginning of the optimization and then gradually increased throughout the iterative cycles to further penalize the intermediate density elements. The penalization factor can however be set to a fixed value if preferred.

3

Requirements and set-up

This chapter will explain the requirements on the crossmember as well as the constraints on the component. Further, the general set-up for the optimization will be discussed.

3.1 Loads and fasteners

Three different load-types will be included in the optimization method for this thesis. Figure 3.1 illustrates the crossmember (grey) and connecting side brackets (red) and engine mounts (blue). It is assumed that the torque rods absorb all moments from the engine, and thus they are excluded from the input loads.

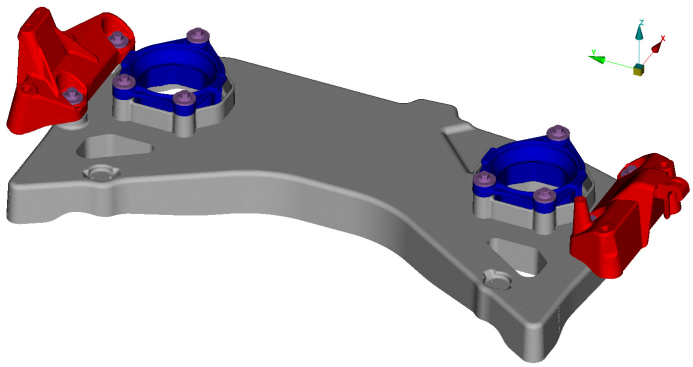

Figure 3.1: Overview of the crossmember design space with connecting mounts and brackets.

The different load cases on the engine mounts are listed in table 3.1. Each load case consists of a maximum or a minimum load in a certain direction. The engine load is distributed in the engine mounts via RBE3 connections. A RBE3 connection is commonly used to apply a load on a surface. The load is applied on a dependent node with three translating DOFs, the dependent node distributes the force on the connecting reference nodes. Unlike the RBE2 element, the RBE3 element does not add an artificial stiffness to the structure.

Table 3.1: The six different load cases on the right and left hand engine mounts. The magnitude has been scaled for confidentiality reasons.

		LHM	RHM
X-positive	[N]	2.7	2.0
X-negative	[N]	-3.0	-2.2
Y-positive	[N]	1	1.1
Y-negative	[N]	-1.4	-1.3
Z-positive	[N]	2.1	1.4
Z-negative	[N]	-6.2	-4.5

In this thesis, three different crash scenarios have been implemented, where the first crash scenario is divided into two subcases on each side of the crossmember. They will be referenced as *crash 1 left*, *crash 1 right*, *crash 2* and *crash 3*. Crash 1 is presented in figure 3.2, and crash 2 and 3 is presented in figure 3.3.

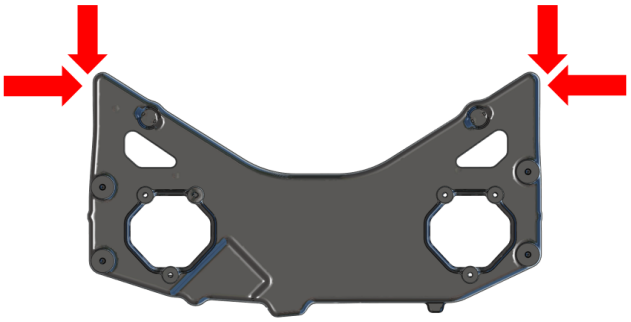

Figure 3.2: Illustration of crash scenario 1. Note that the loads on the left and right side are applied in two separate load cases.

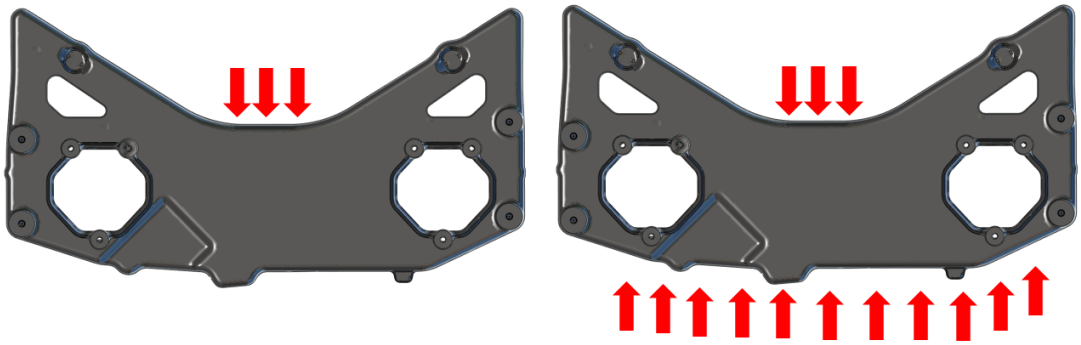

Figure 3.3: Illustration of crash scenario 2 (left) and crash scneario 3 (right).

The crashes generates high loads on the crossmember. These loads are of impact character, they are very large but only acts under a short period of time. The

contact area is estimated from visualization of a crash simulation and the loads will be distributed evenly over the area with RBE3 elements. The magnitude of the forces are given from crash simulations and are significantly larger than the engine loads.

The road induced loads will enter the crossmember via the screw connections on the side brackets. The road induced load arises from driving over rough terrain or larger obstacles on the road they will be incorporated in the optimization model via superelements. They will be applied in the spring tower of the BIW.

3.2 Requirements on crossmember

In addition to absorbing loads generated by the engine, the crossmember has some additional vital functions. Because of its size, its behaviour during crashes is of great importance. Certain rigidity of the crossmember is important to make sure it behaves properly throughout the crash. As engine loads are less extreme, the effective stress should not be above the yield stress of the material when these forces are exerted on it. Exceptions can be made if the high stresses are local.

3.3 Superelement

Running a full FEM-analysis multiple times can be costly and slow, furthermore, if an error occurs somewhere in the model, there is a risk that the whole simulation fails. To significantly reduce computational cost while still retaining a high accuracy, a so called superelement will be used. The use of a superelement can reduce the computational cost with 2-30 times compared to running a regular FE analysis [Siemens, 2014]. A superelement is previously calculated solution that can be reused without rerunning the whole simulation. The purpose is to be able to exclude almost all surrounding components from the optimization process but still get realistic loads and reactions from them. For each connecting node, the superelement returns a reduced stiffness matrix which is then used in the optimization model.

The superelement used in the thesis represents the BIW of the front half of the car, shown in figure 3.4. It will connect to the optimization model through beam elements which represent the screws joining the crossmember with the side brackets. As such, there will be four connections between the superelement and crossmember. Additionally, the superelement can incorporate loads and different boundary conditions. This will be used to model the road induced loads which propagate through the spring towers of the BIW. The side brackets connecting crossmember with the BIW are included in the superelement to increase the computational efficiency. If the side brackets would be included in the optimization model, a total of seven ASETs would be needed, contrarily, modelling the M12 screws and connecting them to the superelement reduces the number of ASETs to four. An ASET can also be created to apply a load or a displacement on the superelement.

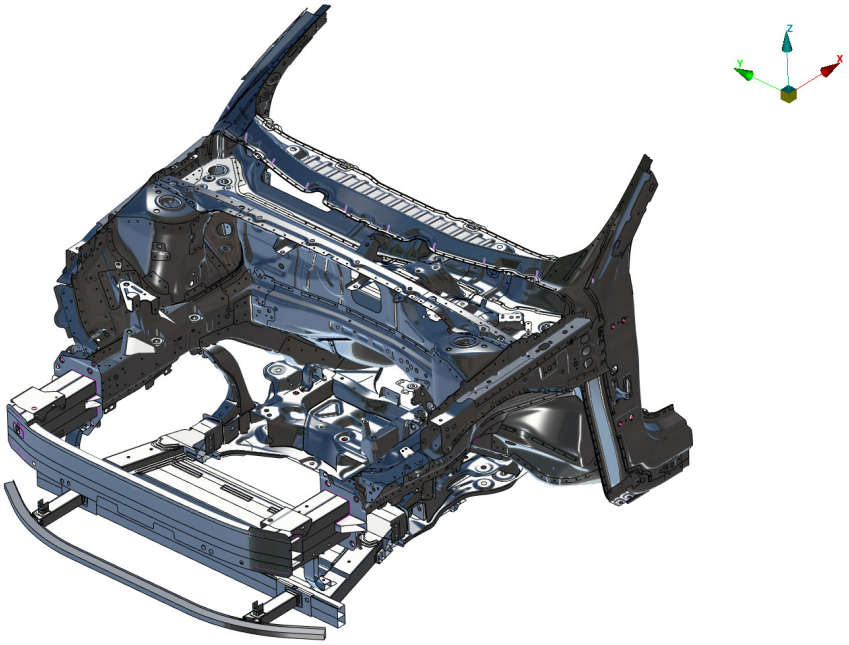

Figure 3.4: Representation of the BIW which is reduced to a superelement and used in the optimizations.

3.4 Manufacturing Constraints

The crossmember is manufactured through *High Pressure Die Casting* (HPDC). HPDC can produce complex geometrical structures and the casting method can locally manufacture sections thinner than 1 mm [OpenLearn, 2017]. HPDC uses a die split in two section, in the beginning of the casting process the die is pushed together. Afterwards, the molten metal is released into an injection barrel and pressed into the die to ensure that there is not any air inside of the mould. When the material has hardened, the die opens and the component is pushed out by ejector pins. HPDC is often used to cast non-ferrous metals such as zinc and aluminium.

In OptiStruct, casting manufacturing constraints can be implemented by specifying a so called *draw direction*. The draw direction tells OptiStruct that material can only be drawn from a certain direction, which makes it unable to create holes perpendicular to the draw direction. To establish feasibility in a manufacturing point of view, this setting will be used in all optimization runs. Though to ensure a component that has good manufacturing properties, some post processing must always be performed. Most important to ensure good manufacturability is to have as similar thickness as possible on all parts of the component.

3.5 Material

The crossmember is made of a highly ductile aluminium alloy, and some important material properties parameters are presented in table 3.2.

Table 3.2: Material data for the crossmembers aluminium, where σ_y is the yield stress, σ_u is the ultimate stress, ε_f is the fracture strain, ρ is the density, E is Young's modulus and ν is Poisson's ratio.

σ_y	σ_u	ε_f	ρ	E	ν
120 MPa	200 MPa	12 %	2700 kg/m^3	70 GPa	0.3

3.6 General optimization set-up

Multiple settings for the optimization will be used in this thesis to evaluate different approaches but some settings will remain the same for all cases. The model contains ten screw connections, four M12 screws connecting the crossmember with the body brackets and six M10 screws joining the engine mounts with the crossmember. The M12 screws will be modeled with RBE3 and beam elements, to ascertain connection to the superelement. To enable the possibility to include pre-tension, the M10 screws will be modeled with solid elements. There are three contact locations that require contact settings, see figure 3.5. The first contact is between the screw head and the engine mount, second contact is between the engine mount and the crossmember and lastly, there is a contact inside the screw hole between the crossmember and the screw.

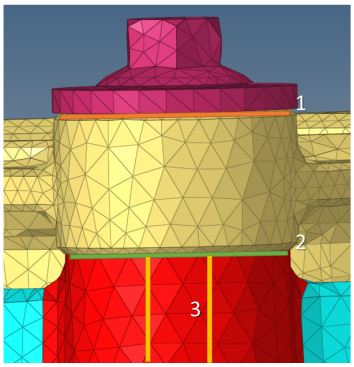

Figure 3.5: The three contact locations around the screws.

Sliding will not occur in the first and third contact and hence a so called *tie* or *freeze* contact is used. This contact type will colligate the two pertaining surfaces. The second contact can be specified in two different ways, either a freeze contact can be chosen or one can allow sliding. Sliding is chosen if a pre-tension is applied on the

screw. A sliding connection also requires a correct friction coefficient between the two components as it is material dependent.

Certain parts of the crossmember have specific purposes and can therefor not be removed. For example, the screw holes need to remain and the two immersions at the front of the crossmember are there to connect electrical components to and through the crossmember. Hence, the design space need to be chosen carefully. The full design space is shown in figure 3.6. For the purpose of optimization the additional parts on the crossmember is removable as they do not add any significant stiffness to the component.

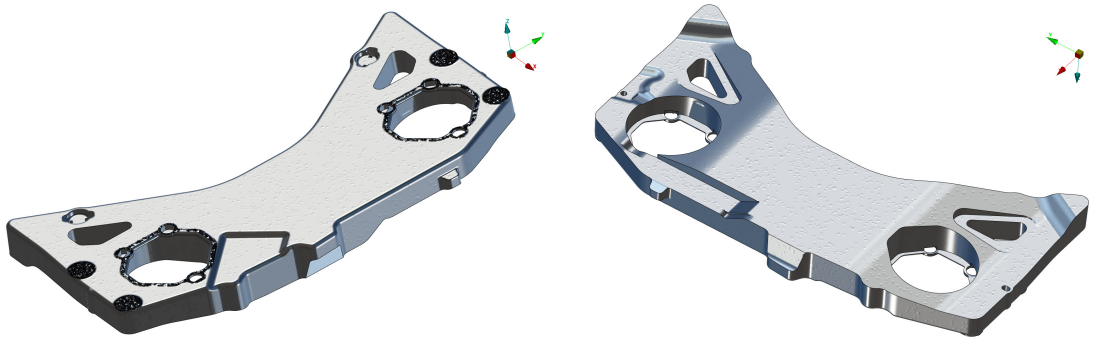

(a) Top side of the design space. **(b)** Bottom side of the design space.

Figure 3.6: Illustration of the design space used in all optimizations.

3.6.1 Weight

A target weight is needed when minimizing compliance, which is in this case based on the weight of the current crossmember. The target mass fraction was calculated to 28%. Additionally, to ascertain manufacturability it is estimated that some 30% extra weight is needed after optimization. As such, some trial cases has included this constraint which lowers the total mass fraction to 20%. Volume fraction has been used instead of mass fraction since the crossmember is made from a homogeneous material.

3.6.2 Reanalysis of optimized model

Viewing the results of an optimization can be a bit misleading since the element densities varies from $0.3 < \rho < 1$. The reason for this is that elements with a density less than 0.3 has been removed as they have a negligible stiffness. A reanalysis with solely solid element is needed in order to get a more accurate result of the optimized crossmember's properties. OptiStruct has the function OSSmooth that smoothen surfaces and creates a new geometry from an optimized model which the function remesh automatically. A drawback is that OSSmooth can not capture the

exact geometry of the optimization and it often slightly enlarge the rib structure. Also the element quality can be somewhat poor and surfaces can be locally rough. Nevertheless, the results will better resemble a fully optimized and manufactured crossmember.

4

Results

This chapter will present the set-ups and results from different optimization runs. The optimizations minimize the compliance and use a pre-calculated value for the sought volume fraction.

4.1 FE analysis of existing component

An FE analysis of the existing crossmember has been done to have a benchmark to compare the optimized component to. The compliance of the crossmember is of particularly interest since it can be directly compared with the optimized model's compliance. An analysis of the existing component also gives a better understanding of how the stress distributes and how it deforms in different load cases. The most interesting load case results will be presented in the end of this section.

The analysis of the existing crossmember uses a superelement to resemble the BIW to get an accurate reflection of the stiffness of the surrounding components. The loads will be placed on the same regions, with the same magnitude as in the optimization model and as for the optimization model, ten different load cases will be investigated. The simulation setup is summarized in table 4.1.

Table 4.1: Simulation configuration of the existing crossmember.

Type	Linear Static
Mesh type	Second order tetrahedrons
Number of elements	1 261 060

Figure 4.1 and 4.2 illustrate the von Mises stress distribution on the crossmember during crash 1 on the left side, as the first crash load cases are the most severe. As expected, the stresses are high in multiple areas. The crossmember will plasticize during crash 1 due to the severe strain the component is subjected to. In figure 4.1 it can be seen that multiple ribs close to the load locations are under extreme stress and in figure 4.2 the material surrounding the bracket screw holes shows high stress concentrations. Overall, it can be noted that the stress is non uniform and that stress concentrations are found in local regions.

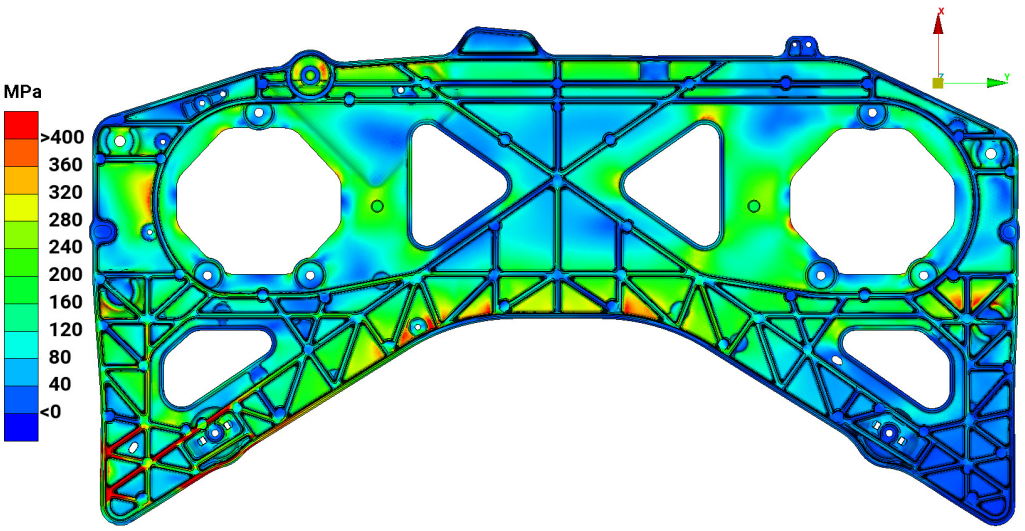

Figure 4.1: von Mises stress distribution on the bottom side of the crossmember during crash 1 on the left hand side.

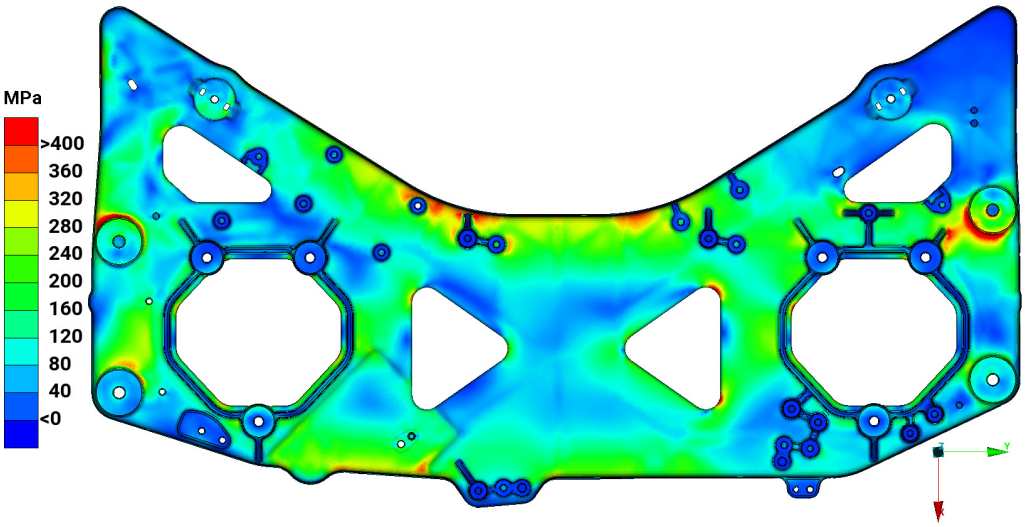

Figure 4.2: von Mises stress distribution on the top side of the crossmember during crash 1 on the left hand side.

The Z-negative engine load is the largest load and it is therefore important to investigate the stress in critical regions for this case. Figure 4.3 shows the stress around the left engine mount and screw holes connecting the side brackets. The material is close to yielding in the areas surrounding the screw holes. The stress was also locally above 100 MPa in one of the ribs on the bottom side.

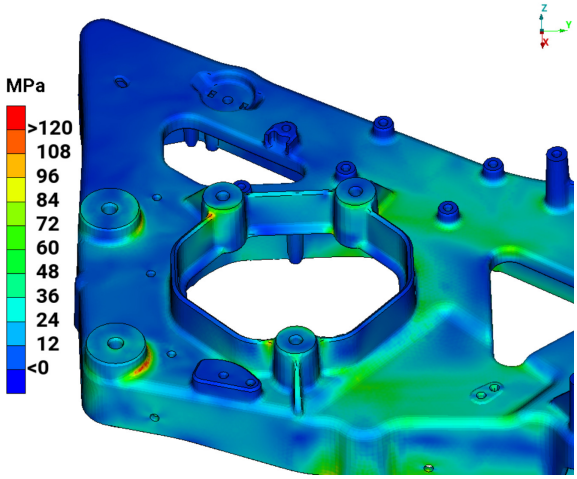

Figure 4.3: von Mises stress distribution of Z-negative load case. In some local areas the yield stress of the material is exceeded.

It is also of interest to investigate the strain for various cases. In table 4.2 the maximum von Mises strain is tabulated.

Table 4.2: The maximum von Mises strain for the different engine load cases.

X-positive	7.39E-4
X-negative	8.14E-4
Y-positive	2.97E-4
Y-negative	3.77E-4
Z-positive	5.47E-4
Z-negative	1.39E-3

For the load cases in the X and Y direction, the strains are largest in the engine mounts. When the engine loads are applied in the Z direction the strains are largest on ribs on the back side of the crossmember. The reason is that the crossmember bends and the centre of the crossmember displaces vertically. Since the set-up is a linear static analysis, the maximum strain for the crash cases are considered to be non-physical and will thus not be compared with the optimized models.

The compliance for the load cases with largest loads are presented in table 4.3. It will be of interest to compare the compliance of the existing crossmember with optimized models since it gives a good indication of how stiff the component is.

Table 4.3: The compliance of the existing crossmember for the largest load cases.

	Crash 1 left	Crash 1 right	Crash 2	Z-negative
c [mm/N]	2.36E+6	2.28E+6	1.8E+5	4.01E+4

4.2 Variables and parameters in OptiStruct

A wide range of variables and parameters are available in OptiStruct to specify the optimization problem. Every optimization requires an objective to optimize with

respect to, usually chosen as minimization of the compliance. Further, one or several constraints can be applied to the design space, for example a maximum allowed mass or volume.

Multiple parameters are offered to refine the optimization. MINDIM and MAXDIM controls the minimum and maximum thickness of members that can be formed during an optimization. An important setting when it comes to manufacturability is MIN GAP which allows the user to control the minimum distance between ribs. Another manufacturing parameter is labeled DRAW. It is a casting parameter which specifies in what direction the die is filled in the casting process, the parameter further allows the user to specify if holes are allowed in the design space. A checkerboarding filter is always applied to ascertain solutions without checkerboarding, and is a default setting in OptiStruct.

4.3 Optimization runs

Many trial runs have been conducted which will not be presented in this thesis. The knowledge gained from them has been utilized to make informed decisions in further optimization runs. As the optimization uses static and linear implementation of the crash loads, the values of the stresses are not valid for these loads but the distribution and comparison to the current crossmember are of interest.

4.3.1 Standard settings

The standard settings for all simulations is presented in table 4.4 and 4.5. If nothing else is specified, these settings are used throughout this chapter. All simulations are run on 16 cores to enable comparison of computational time.

Table 4.4: Basic simulation configuration.

Type	Linear static
Mesh type	First order tetrahedrons
Number of elements	15.179.694
Average element length	2 mm

Table 4.5: Basic simulation configuration - optimization settings.

Parameter	**Setting**	
Objective variable	Compliance index	[mm/N]
Target volume fraction	28	[%]
MINDIM	4	[mm]
MAXDIM	10	[mm]
MINGAP	30	[mm]
DRAW	Z-direction	[-]
NO HOLE	TRUE	[-]

4.3.2 Case 1 - Standard settings

Case 1 does not deviate from the settings described in section 4.3.1. The rib structure generated in this case is presented in figure 4.4. As expected, material is prioritized

to account for the loads from crash 1. These settings created ribs with a thickness varying from 4 to 10 mm. The required CPU time for this case was 419 hours.

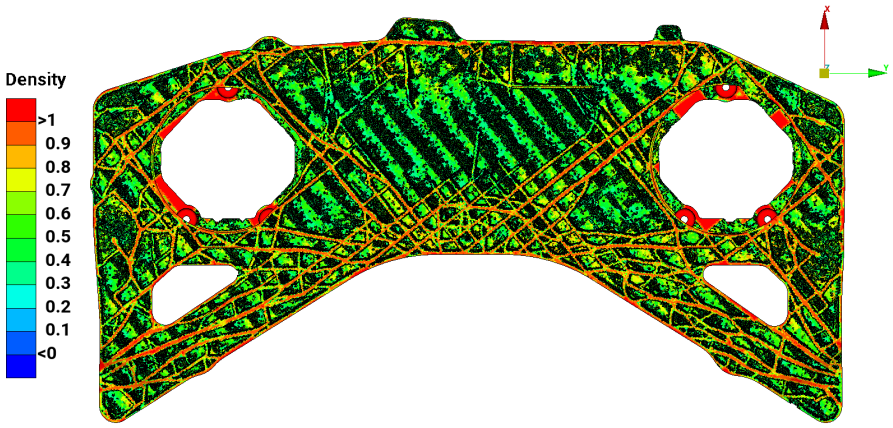

Figure 4.4: Rib structure of the standard case.

The compliance for the load cases of the optimized model is presented in table 4.6. As the crash 1 load cases have a significantly larger compliance than the rest, the model is primarily optimized to these. The compliance is slightly larger than for the existing crossmember, but this is due to that a large proportion of the elements has a density $\rho < 1$. A reanalysis is required to compare compliances between an optimized model and the existing crossmember.

Table 4.6: Compliance case 1.

Load case	**Compliance** [mm/N]
Crash 1 left	2.50E+6
Crash 1 right	2.37E+6
Crash 2	2.08E+5
Crash 3	6.07E+4
Z-negative	5.19E+4
Other engine loads	1-5E+3

Figure 4.5 shows the effective stress distribution from crash 1 loads. The magnitude of the stresses are comparable to the existing crossmember. Notably, the bottom side of the crossmember plane seems to have low stresses. This is due to those elements having a density $\rho < 1$, which effectively reduces their stiffness. If a reanalysis is done, these elements would have full density, and thus the stress along this plane would be distributed more evenly through the thickness, resulting in a stress magnitude approximating the one of the existing crossmember.

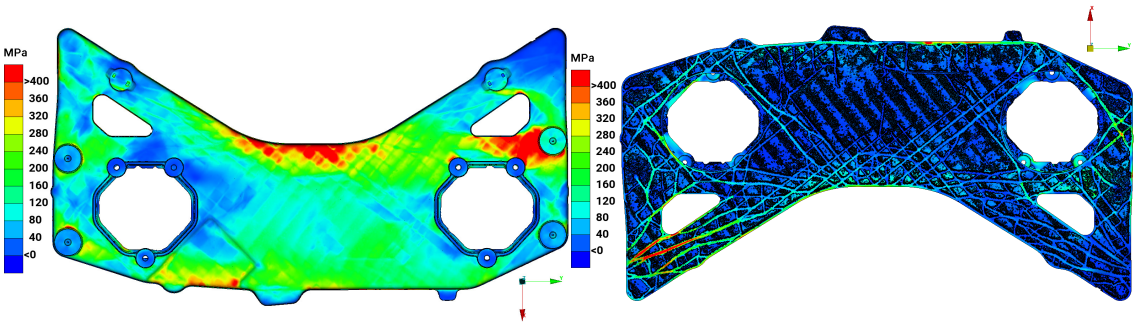

(a) Top view. **(b)** Bottom view.

Figure 4.5: von Mises stress distribution in left crash 1 load case.

It is of interest to look at some other load cases as well. None of the engine loads give stresses above the yield stress of the material with the exception of negative Z, shown in figure 4.6. As can be seen, local areas such as in the vicinity of the engine mount and bracket screw holes exceed the yield stress. Also, its compliance is one order of magnitude larger than the other engine loads. It seems as the component lack horizontal ribs between the lower side of the engine mounts, which would increase the bending stiffness in Z-negative load case.

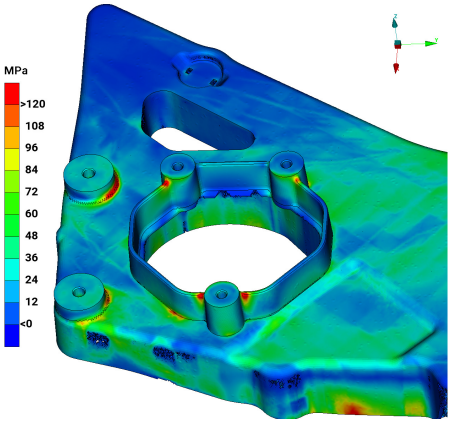

Figure 4.6: von Mises stress distribution of Z-negative load case. Some local areas exceed the yield stress of the material.

Figure 4.7 shows the von Mises stress distribution from the crash 2 load case. The most surprising result with this load case is the absence of vertical ribs in the center of the crossmember. As the stresses are quite large and with the current angle of the ribs, and considering the possibility of large plastic deformations, this design might be susceptible to failure if the crash 2 load contact area deviates from the set-up here.

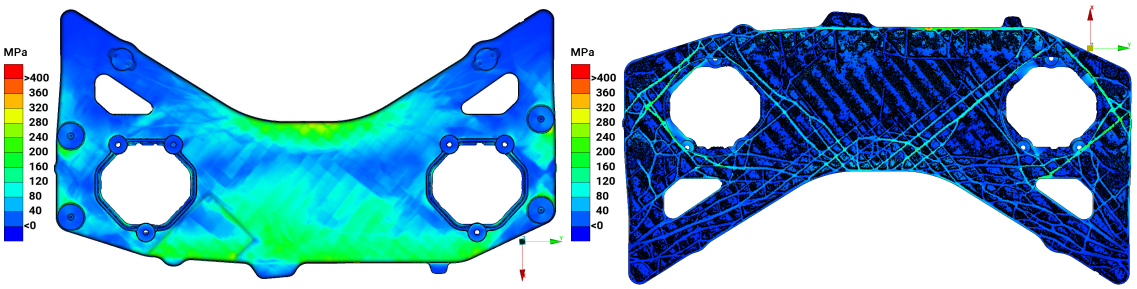

(a) Top view. **(b)** Bottom view.

Figure 4.7: von Mises stress distribution in crash 2 load case.

The stress distribution for the reanalyzed model is shown in figure 4.8. The stress is generally more evenly distributed across the crossmember and the number of regions with a high stress concentration is considerably lower compared with figure 4.5. In this figure the element density varies which can be compared with the existing crossmember in figure 4.1. It can also be seen that the regions with a high stress factor for the Z-negative load case is lower on the reanalyzed model, this is shown in figure 4.9.

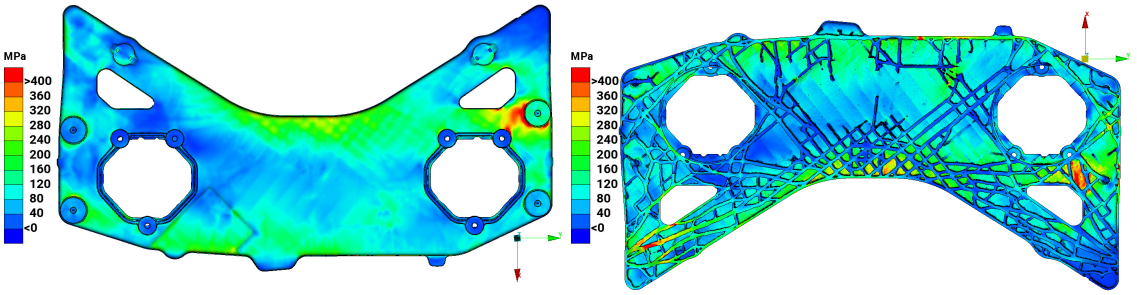

(a) Top view. **(b)** Bottom view.

Figure 4.8: von Mises stress distribution in left crash 1 load case for the reanalyzed model.

Comparing some of the compliances for the reanalyzed model in table 4.7 with compliance after the optimization (table 4.6), it can be seen that the compliance is lower for all load cases. The result is expected since the reanalyzed model is somewhat bulkier. More interestingly, the compliance can be compared with the existing crossmember (found in table 4.3). The compliance is higher for the three crash loads in the existing crossmember while Z-negative is higher for the reanalyzed optimization. The Z-negative compliance is larger after the optimization since the

compliance index will focus on minimizing the compliance for the crash cases since they are significantly higher.

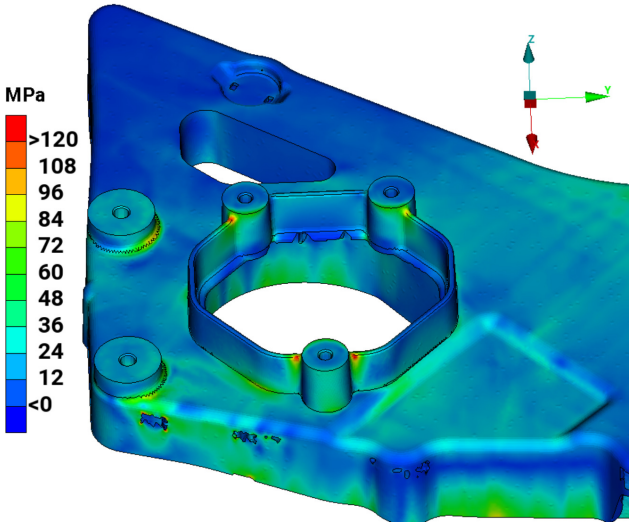

Figure 4.9: von Mises stress distribution of Z-negative load case on the reanalyzed model. Some local areas exceed the yield stress of the material.

Table 4.7: Compliance for the reanalyzed model.

Load Case	Compliance
Crash 1 left	2.27E+6
Crash 1 right	2.12E+6
Crash 2	1.48E+5
Z-negative	4.45E+4

4.3.3 Case 2 - No member size control

In this case, MINDIM, MAXDIM and MINGAP are turned off, allowing for structures of any thickness. Draw direction is still on to ensure manufacturability, but the integrity of the created structures can be discussed. The reason for this optimization is to see where material is most needed. Only one rib exists at the topside, but it is significantly thicker than 10 mm, with increasing thickness close to the crossmember plane. Figure 4.10 shows the structure of the component when using these settings. The material is located at similar locations as for the standard settings, but now as no constraint on the size of the ribs then only few large and thick ribs are created. The CPU-time for this case was 160 hours which is significantly shorter than the other cases.

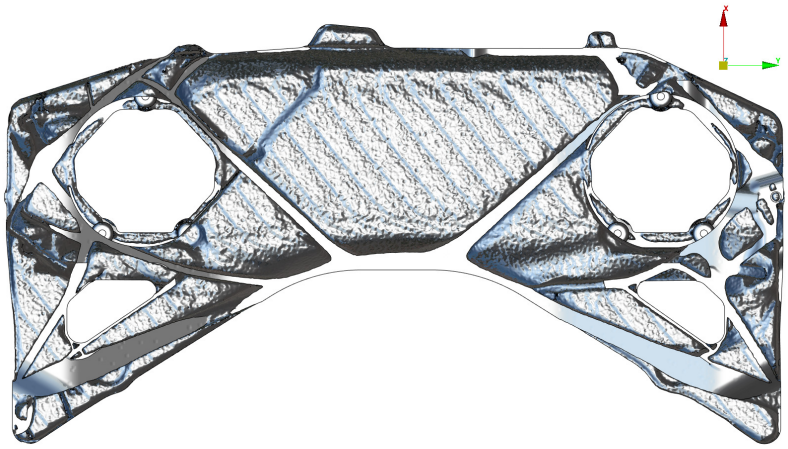

Figure 4.10: Rib structure with no member size control. Rendered graphics to enhance visualization.

Figure 4.5 shows the von Mises stress distribution of load case crash 1 left. Due to the size of the ribs, the stresses are much lower, they almost does not surpass the ultimate stress of the material. The weak points are still the bracket screw holes, specifically the one on the opposite side of the crash load.

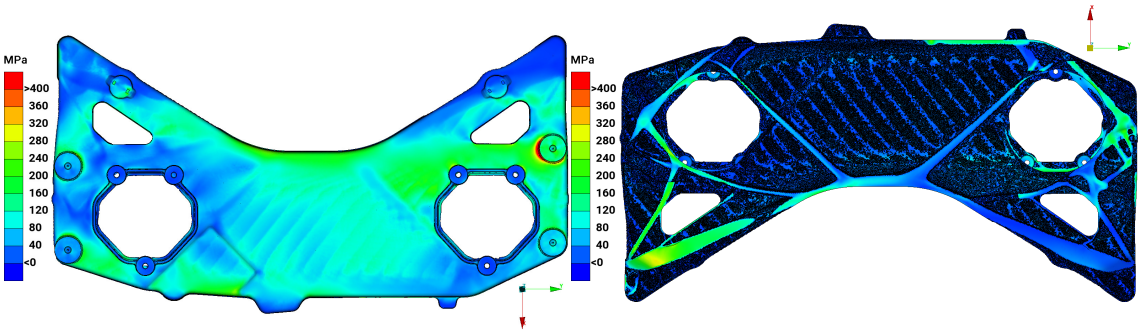

(a) Top view. **(b)** Bottom view.

Figure 4.11: von Mises stress distribution in left crash 1 load case.

As with the standard settings, this model still has problems with the Z-negative load case, albeit slightly less so. The problem areas remain the same, and the magnitude of the stresses there are similar or slightly lower. The same applies for the rest of the model, all stresses are somewhat reduced.

The compliances, listed in table 4.8, have similar relative magnitude to each other but are mainly lower than that of the standard settings. This is expected as the settings are overall the same, but this case has fewer constraints. As such, the optimization algorithm has more freedom to create a more optimal structure. However considering manufacturability, the quality of the material would be significantly worse than the existing crossmember, and most likely the entire upper plane of the crossmember would bend during the cooling process as it is much thinner than the ribs. Thus, these settings can indicate where material is most needed and based on this ribs with uniform thickness could be manually created.

Table 4.8: Compliance case 2.

Load case	**Compliance** [mm/N]
Crash 1 left	2.23E+6
Crash 1 right	2.19E+6
Crash 2	1.52E+5
Crash 3	7.79E+4
Z-negative	4.78E+4
Other engine loads	1-5E+3

4.3.4 Case 3 - Lower volume fraction

Here the volume fraction constraint is lowered from 28% to 20% to grant a margin for weight increase to account for manufacturability. The rib structure in this case is presented in figure 4.12. Most ribs on the topside of the crossmember have disappeared, but the appearance of a rib running vertically in the center of the crossmember can be noted. The CPU-time was 389 hours, which is slightly less than for the case with 28% volume fraction.

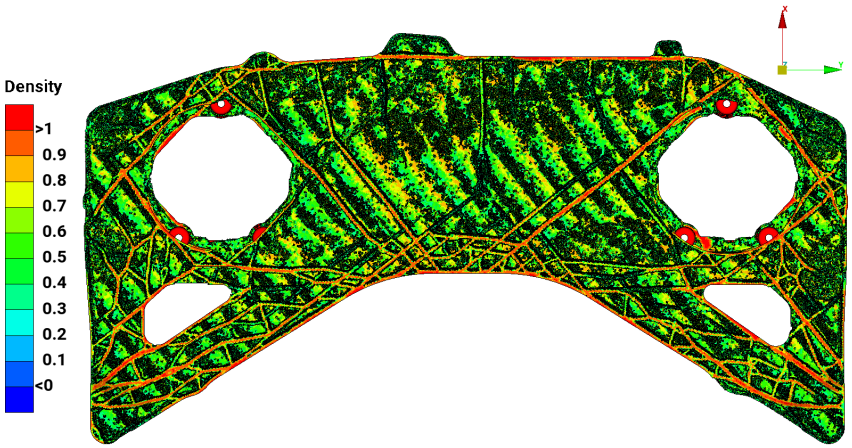

Figure 4.12: Rib structure with 20% volume fraction.

The compliance is presented in table 4.9. Compared to standard settings, the compliance is larger for every case. As more material is removed, this is not surprising. The relation between the different load cases is similar to the standard settings.

Table 4.9: Compliance case 3.

Load case	**Compliance** [mm/N]
Crash 1 left	2.55E+6
Crash 1 right	2.42E+6
Crash 2	2.36E+5
Crash 3	8.30E+4
Z-negative	5.49E+4
Other engine loads	1-5E+3

Figure 4.13 shows the stress distribution of the von Mises stress in crash 1 left load case. The magnitude is slightly larger than for the standard case, but the similarity indicates feasibility to handle crash 1 as intended.

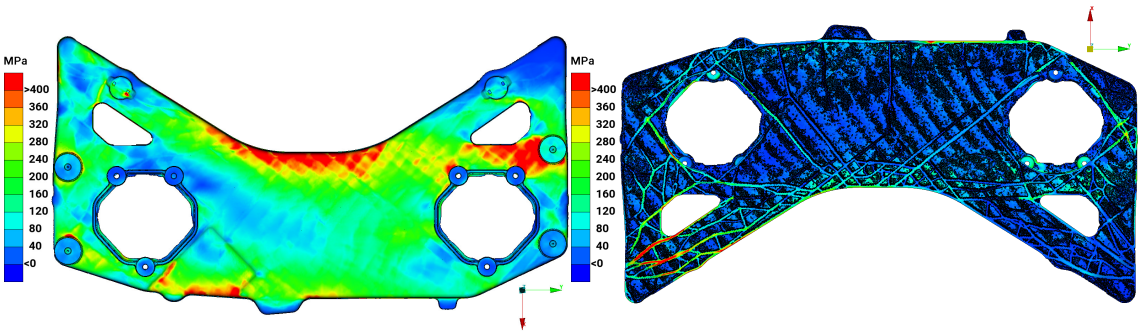

(a) Top view. **(b)** Bottom view.

Figure 4.13: von Mises stress distribution in left crash 1 load case.

Not surprisingly, the Z-negative load case (figure 4.14) shows similar but larger problems than the higher volume fraction case. As such, the already limited material would need to relocate to accommodate for this load case, which in turn would worsen the performance of the other load cases. But compared to the existing crossmember, there is still more material in the vicinity of the crash 1 impact zone, which indicates that there is room for this adjustment while still performance is kept for the crash 1 load case.

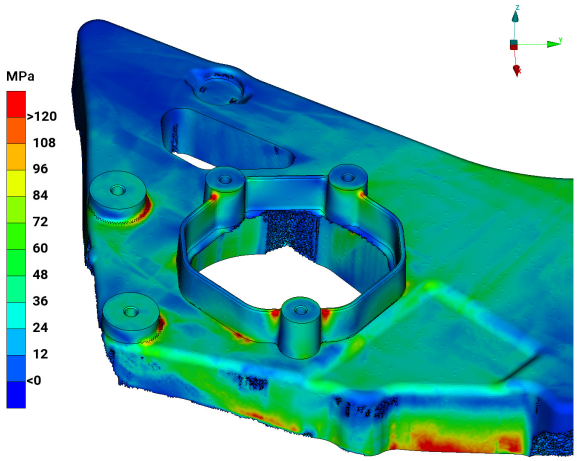

Figure 4.14: von Mises stress distribution of Z-negative load case.

4.3.5 Case 4 - Weighted load cases

With the settings used in the previous cases, OptiStruct tries to minimize the sum of compliance for all load cases. Thus the load cases with the largest compliance will dominate the optimization while less consideration is taken to the load cases with a smaller compliance. The optimization seeks a structure with the lowest sum of compliances, and a reduction of compliance in the load case with greatest compliance will influence the total compliance the most. Generally this is desirable as the load cases with the largest compliance usually are the cases which dimension the component most. In our model though, the crash loads do not have to confine below the yield stress, while the engine loads strive to do so. This means that the optimization has to take the load cases with a stress constraint into greater consideration and a way to do this is by amending the weight factors. In earlier cases, the optimization has struggled to comply with the stress levels in Z-negative load case. Using the compliances from table 4.6, an estimation of the weight factors is derived. Due to the magnitude of the compliances in crash 1 load case, a decision was made to reduce the weight factor of these to increase the influence of all other load cases. Additionally, the Z-negative load case weight factor was increased.

Table 4.10 lists the compliances from the standard settings optimization and the weight factors. From those estimated compliances are calculated, which represent what the weighted compliance would be with the structure generated with the standard settings. Finally, the actual weighted compliances are shown, which are calculated from the optimized model using the listed weights. An increase compared to the estimation means that the load case is less optimized to, and a reduction means that the load case is taken into greater consideration.

Table 4.10: Compliance case 4.

Load case	c **in standard**	W	**Estimated** $W \cdot c$	**New** $W \cdot c$
Crash 1 left	2.50E+6	0.2	5.00E+5	5.06E+5
Crash 1 right	2.37E+6	0.2	4.74E+5	4.83E+5
Crash 2	2.08E+5	1	-	1.92E+5
Crash 3	6.07E+4	1	-	3.56E+4
Z-negative	5.19E+4	2	1.04E+5	1.01E+5
Other engine loads	1-5E+3	1	-	1-5E+3

The general structure is similar to not using weight factors, but there are some differences. An overview of the entire rib structure can be found in appendix A.1. The ribs close to the crash 1 impact zone are a bit more scarce, and the ribs are somewhat thinner there. A large difference is the structure in the middle and middle-top, shown in figure 4.15. Now there is an additional structure which goes horizontally close to the top. Also there is an additional rib which goes from the center bottom at an angle upwards on each side, as well as two vertical ribs in the center. These changes seem to accommodate for crash 2 and 3, which is reflected in the substantial decrease of compliance for these load cases. The changes in rib structure would also increase the bending stiffness for Z-negative load case.

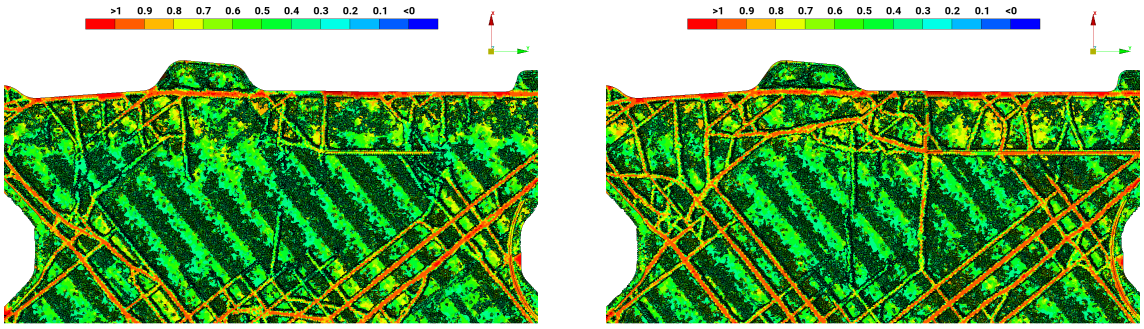

(a) Standard settings. **(b)** Altered weights.

Figure 4.15: Comparison of the rib structure between the standard case and weight case. Zoom on the top side of the crossmember.

Figure 4.16 shows the von Mises stress distribution for the Z-negative load case. The stress in the problem areas is reduced by about 10%, and there is no yielding of the material in the vicinity of the bracket screw holes. Thus the weighting worked in the intended way, by causing the Z-negative load case to have a larger role in the final design and reducing the stresses in that load case.

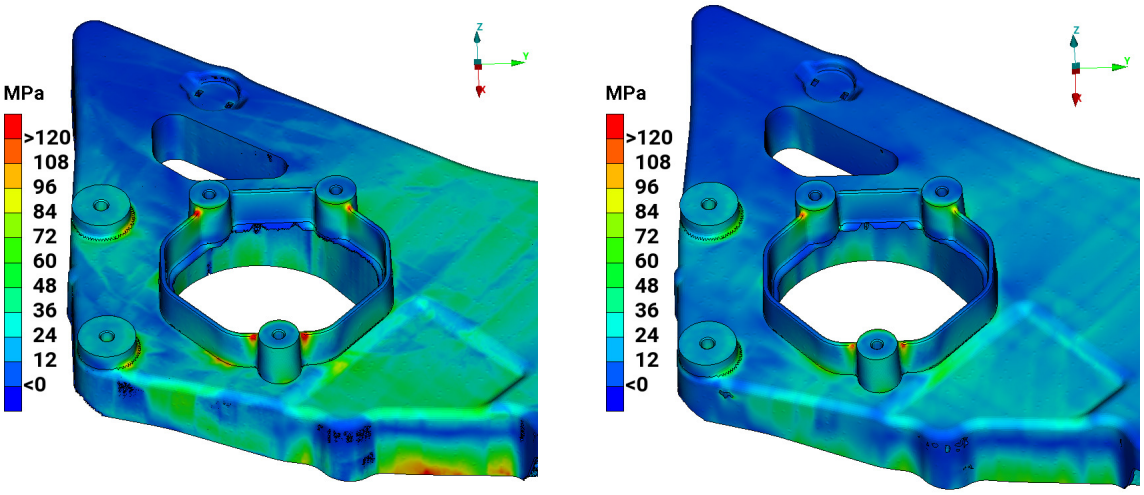

(a) Geometry without a reanalysis. **(b)** Reanalysed geometry.

Figure 4.16: von Mises stress distribution of Z-negative load case on the optimized and reanalysed model.

4.3.5.1 Discussion

Setting up good weight factors is no easy business. First of all, it requires a baseline optimization to get compliances to work with. It is very difficult to estimate the magnitude and relation of the compliance without running an optimization first. Thus, weights would be a secondary step to fine-tune an optimization if some problem arises, as with the Z-negative load case here. Even so, choosing weight factors which desirably improves the structure is not easy. In this case Z-negative weight factor was set to 2, and even with lowering crash 1 weights there was not an immense improvement of Z-negative load case as the compliance was only lowered by 3%. As there still existed areas with stresses above the yield stress, perhaps the weight factor should have been set to 3 or 4, or some other value above 2. Additionally, the decision to lower the crash 1 weight factor can be questioned. The idea was to increase the significance of Z-negative and crash 2 and 3 loads, but it might have been better to only increase the weight of those cases instead.

Another way to influence the weighting of load cases is to change the values of the loads themselves. This would prevent the ability to read stresses or other results directly from the optimization, thus requiring a reanalysis. The advantage however is easier predictability of the optimization.

4.3.6 Case 5 - Divided crash load

An aspect of the set-up for the optimization is how and where the loads are applied. Data given from the crash department shows how large the crash loads over a specific region are but it does not clarify where in the region the peak load is exerted. To investigate how the application of the crash 1 loads influences the optimization, the crash 1 loads were divided into to regions which are illustrated in figure 4.17. 70%

of the load was placed in the first region whilst the 30% of the load was placed in the second. The largest load was applied in the first region since the sidemember first comes in contact with that zone. The elapsed CPU time for the optimization was 328 hours.

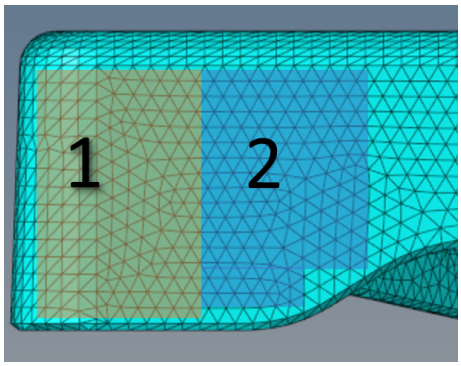

Figure 4.17: An illustration of how the crash 1 load is divided.

The main purpose of the optimization was to observe how dependent the ribs around the largest loads was influenced by its application, a zoom of the rib structure can be seen in figure 4.18. The rib patterns resemble each other but there are slight differences between them where the largest difference can be found in the top of the figures where the load is applied. It can be seen that the ribs with a divided crash 1 load start to form further towards the corner while with the uniform crash 1 load, the ribs are more concentrated a little further back. As each rib plays a key role under a crash event, a key take away is the importance of knowing how the load is distributed and its magnitude in each region. It can also be concluded that in an early design phase an approximative load region and magnitude are sufficient to get an indication of how the rib structure should be designed.

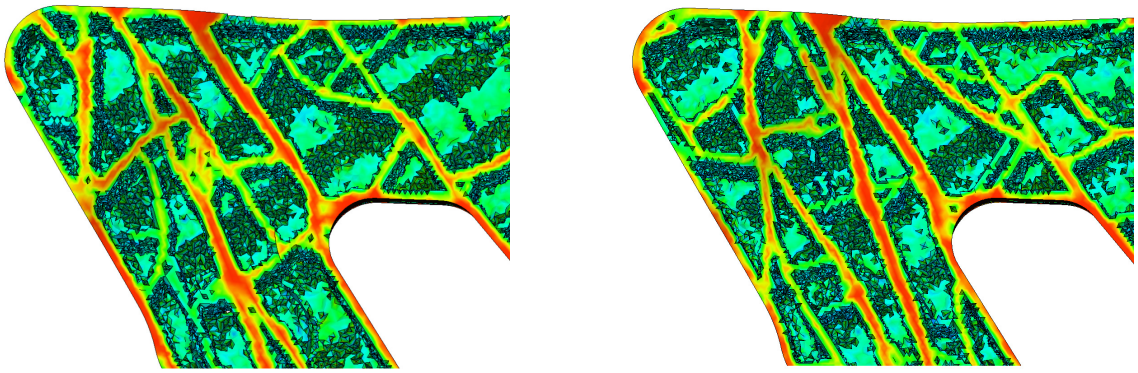

(a) Divided crash 1 load. **(b)** Uniform crash 1 load.

Figure 4.18: The rib pattern around the front left corner for a non-uniform and uniform crash 1 load.

Figure 4.19 shows the stress distribution on the ribs from the divided crash load 1

optimization, with a divided crash load 1 (as depicted in figure 4.17) and with a uniform load in the same area. It can be seen that the results vary depending on how the crash load is applied. The stress is more concentrated to a single region with a uniform load compared with a divided crash where the high stress is more evenly distributed on multiple ribs. In appendix A.2 figures showing the top and bottom side of this optimization indicate that the stresses are higher with a uniform load. It can therefore be said that it is of importance to get as accurate data as possible regarding the crash load to correctly optimize the model for the actual load.

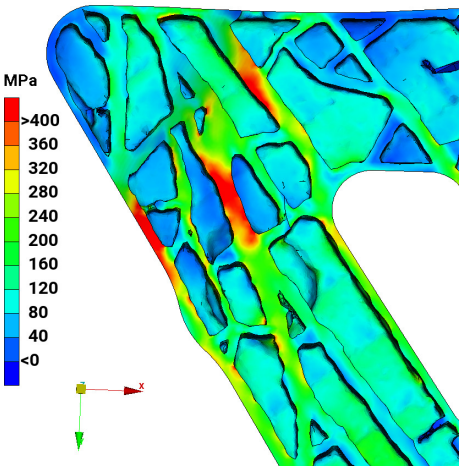

(a) Stress with a Divided crash 1 load.

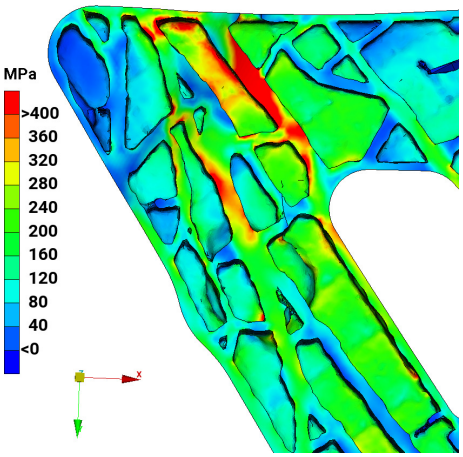

(b) Stress with a Uniform crash 1 load.

Figure 4.19: The rib pattern around the front left corner for a non-uniform and uniform crash load 1.

4.3.7 Case 6 - Road induced loads

Incorporation of road induced loads has been investigated as well. These loads are applied in the spring tower and arise for example when driving over a curb. As the loads are applied to the superelement, modification of it is required. More ASETs are created to be able to apply different loads and boundary conditions which increase the CPU-time. The loads applied in the springtower have a magnitude of 40 kN and are acting in positive Z direction. The CPU-time for this case was 1029 hours, which is more than twice as much as the second longest case.

It is interesting to look at the displacements for the road load case, shown in figure 4.20a. The entire crossmember has a certain rigid body motion, for the right load case the right side of the crossmember translates in Z-direction and rotates around the left hand side. As such, the displacements are very large, but they are a secondary phenomena of deformation of the BIW. Compared to crash load 1, the displacements are close to three times larger for the road induced loads, despite significantly lower stress and strain. To get a more true sense of the displacements without rigid body motion, the strains are advantageously analyzed, shown in figure

4.20b. They display the stretching of elements instead of their displacement, and thus correlate with the stress distribution.

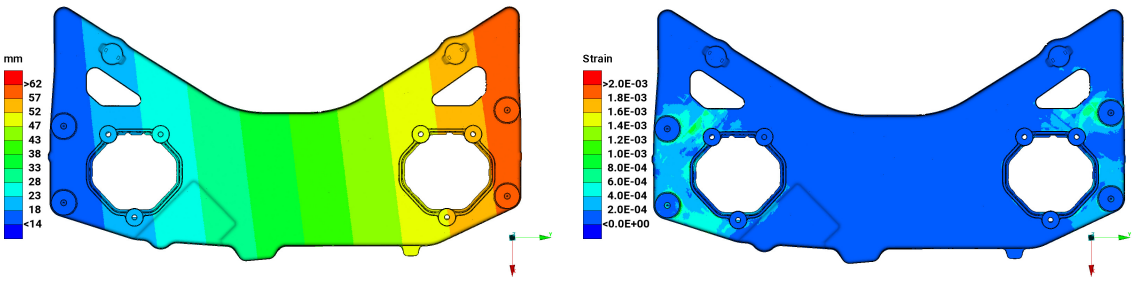

(a) Displacement. **(b)** Strain.

Figure 4.20: Displacement and strain of the road load case.

The compliance, shown in table 4.11, is significantly larger for all cases when incorporating road loads. The road loads themselves are of a magnitude comparable with crash scenario 1. To explain why, we need to remember that the compliance is calculated as displacement times external forces. As said in the previous paragraph, the displacements are very large despite relatively small strains and stresses. Thus this gives a false sense of the stiffness of the crossmember, as the majority of the compliance is caused by rigid body motion. As a consequence the optimization will try to optimize a load case which is not really affecting the crossmember, but rather affects the surrounding structure. Furthermore, the stresses were very low from the road induced loads, which makes optimization in regard to that load case superfluous and counter productive. The result is a poorly optimized crossmember after more than twice the CPU-time.

Table 4.11: Compliance case 6.

Load case	**Compliance** [mm/N]
Road loads	1.56E+6
Crash 1 left	3.03E+6
Crash 1 right	2.96E+6
Crash 2	2.31E+5
Crash 3	6.16E+4
Z-negative	7.35E+4
Other engine loads	2-8E+3

4.3.8 Case 7 - Coarse mesh

In this case the average element size was increased to 6 mm which reduced the total number of elements in the optimization model, and an overview of the altered settings are presented in table 4.12. An implicit problem with this is that the member size constraint has to be updated, as the minimum member size cannot be

smaller than the average element size. Thus the minimum member size was set to 6 mm, and as a consequence the maximum member size was set to 12 mm, as it has to be at least twice the size of the minimum member size. Though this is still not optimal as the recommendation is to set the minimum member size to at least twice the size of the average element size. The CPU-time for this coarse mesh was only 13 hours.

Table 4.12: Coarse mesh set-up.

Parameter	Setting
Number of elements	1.864.799
Average element length	6 mm
MINDIM	6 mm
MAXDIM	12 mm

The optimized model with a coarse mesh is presented in figure 4.21. The main problems are lack of ribs and the ribs tendency to merge together and essentially subvert the MINGAP criteria in some areas. The lack of ribs problem is mainly caused by the increased thickness of the top plane of the crossmember, which restrains the amount of material which can be used for rib structure. The second problem is caused by the lack of space to create ribs, and as such some ribs will merge. Overall though the main layout is similar to the fine mesh, but the casting constraint is not satisfied for this coarse mesh.

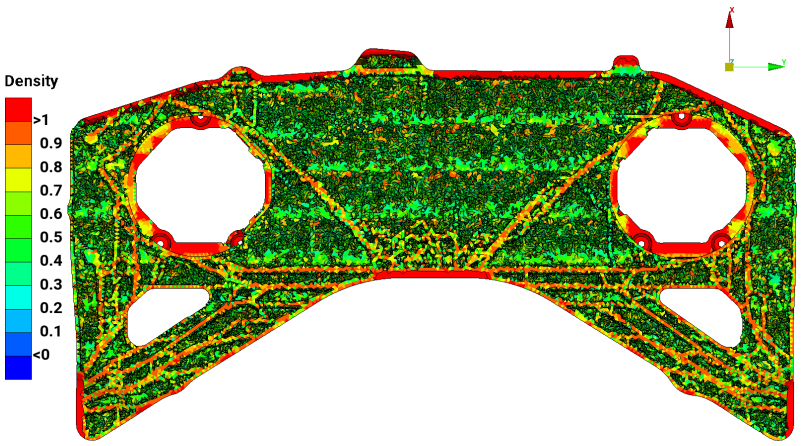

Figure 4.21: Coarse mesh rib structure.

4.3.9 Case 8 - No superelement

In this case the superelement is excluded. The side brackets has thus been included, with solid screws connecting them to the crossmember (see figure 3.1 for an overview of the set-up). The outer screw holes of the bracket have fixed supports. After 100

iterations the optimization had not converged, and convergence in general was a big problem with this set-up. Figure 4.22 shows the generated rib structure when the optimization was terminated after 100 iterations. Most notably there is a lot of clutter of material in the middle, which is most likely due to the optimization's non-convergence. This set-up had a CPU-time of 1042 hours before stoppage.

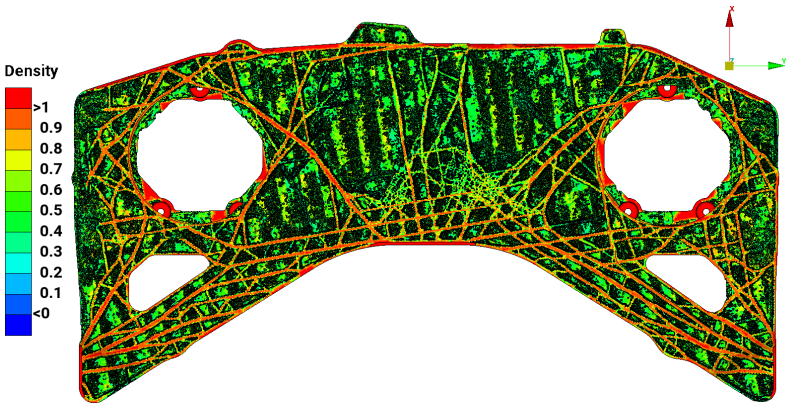

Figure 4.22: Rib structure for model without superelement.

As the bracket outer screw holes are fixed, there is much less movement allowed for the crossmember. This leads to a much stiffer set-up, and the compliance will generally be lower due to this. As a consequence, the compliance can not be compared to any other cases. While the rib structure looks decent, this set-up is not recommended due to the poor assumption of boundary conditions and the massive increase in computational time.

5

Discussion and conlcusion

In this section a discussion regarding the methodology, results, error sources and improvements is given. Lastly, a list of conclusions is presented.

5.1 Results and methodology

Topology optimization with large non-linear transient loads modeled as static linear loads produces promising results when compared to the static linear FE analysis of the existing crossmember. In this thesis it was found that as a tool, topology optimization works excellent in a first stage design to give a good sense of where material is needed and to give non-trivial ideas of how to arrange the ribs. However, although desirable, it does not produce a component ready for manufacturing. Instead it can be used to facilitate early design when information is scarce. If an approximate design space is known and load areas and magnitudes can be estimated, one can come a long way in design just by using topology optimization.

The topology optimization does not only tell where material is needed, it also tells where material is not needed. For example, the areas shown in figure 5.1 do not have any ribs in any of the optimizations. This information is valuable, as holes could be created there to further reduce weight. In some trial cases, it was found that allowing for holes was not a good option, as the entire plane will disappear and left is only ribs. This means that the best option is to not allow for any holes, but instead use the results from topology optimization to find locations where holes can be created afterwards.

The fastest optimization was when no member size constraint was active. It can be useful to do an optimization like that first to identify the most critical areas of where material is most needed. Also, in a case like this where there are different requirements on different load cases, it can help to estimate if weighting is required and the magnitude of the weight for further optimizations. Although it is not manufacturable, it is very easy to do a reanalysis with OSSmooth as the function adds a minimal amount of excessive material due to the simplicity of the rib structure, and thus does not add any significant mass to the model.

In a case like this where there are different requirements on different load cases,

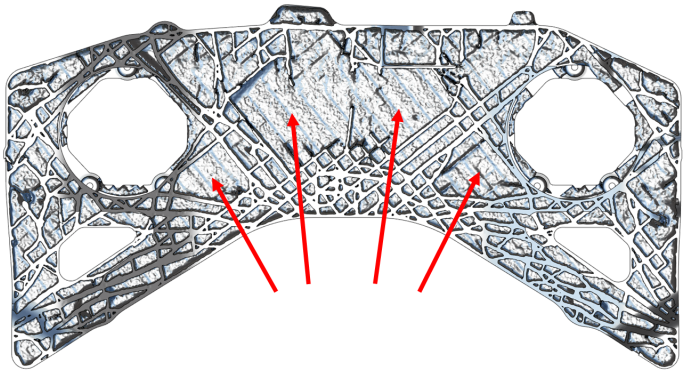

Figure 5.1: Rendered model with standard settings where areas without rib structure are highlighted. These areas lack rib structure in all the results.

implementing weight factors proved a powerful tool. Here we wanted to keep the stresses below 120 MPa for all engine loads, and then increase stiffness for both crash loads as much as possible. There is some difficulty with setting the weight factors to get the desired result however. The weight factors tested in this thesis showed potential in reducing the stress in the engine load case, but they did not get all the way there. However, it could be seen that the stresses above the yield stress for the engine load case did not extend through the thickness as it was concentrated on surfaces. Additionally, some structure near the engine mount screw holes were removed from the optimization model. The removed structure would likely reduce the stress there.

Five of the engine load cases showed considerably lower stresses and displacements compared to the other loads and it was investigated whether it would be more efficient to run an optimization neglecting these load cases. The optimized geometry of that run did not stand out from other optimizations and the CPU-time was not reduced and it was therefore concluded that it is a better approach to include the smaller engine loads. An inclusion of all load cases can be especially important in an early design phase as the magnitude the load can be somewhat uncertain.

The size of the crossmember has brought with it some difficulties. Firstly, a large amount of elements in the design space is required to enable proper manufacturing constraints, which brings with it long CPU-times. Also, the size of the crossmember together with the complexity of the rib structure makes reanalysis a gruesome task.

5.2 Further work and improvements

The different optimization set-ups have shown promising results that can be used during an early design phase but some improvements can be implemented in the process to ensure better results.

5.2.1 Design realisation

After an optimization it is desirable to do a reanalysis of the model, partly to ensure that the results from the optimization is correct but also to be able to investigate other topics, such as durability or non-linearity. The reanalyse in the thesis was done with OSSmooth, which is a built in function in HyperMesh. A preferred approach would be to recreate the optimized design in a CAD software and thereafter run an analysis on the model. In this thesis there was not enough time or resources to realise the optimizations in CAD, mostly because the crossmember is a large complex component which takes a considerable amount of time to accurately recreate in a CAD software. That is why OSSmooth was chosen, despite its limitations.

Functions to constrain the optimization with respect to manufacturability are available in OptiStruct but some alterations are often still needed on the optimized model to make sure that the component can be manufactured with the desired method. The casting constraint also specifies a direction in which no holes are allowed, this can lead to superfluous material in regions which could be removed in a CAD software by a design engineer to save weight.

5.2.2 Crash simulations

The thesis has shown promising results but to validate the methodology the crossmember should be incorporated in a full crash simulation. Comparing the rib structure and the compliance from optimizations with the existing crossmember, the optimized crossmember could show as good or better crash characteristics and it would be interesting to verify it. In order to do so, the geometry needs to be realised as a CAD model and adding back the top parts which was removed from the optimization. A crash simulation would indicate what works well and what parts that need reinforcement or where further material can be removed. The results could later be used to alter the settings in the optimization for the next design iteration or to manually alter the design in a CAD program. The initial plan was to run a full crash simulation with the most promising optimization but unfortunately it was not possible to do so because of a lack of resources.

5.3 Error sources

When analyzing a simulation or an optimization, one always need to consider different assumptions or settings that can lead to uncertainties in the result. The possible error sources that can affect the result will be discussed below.

5.3.1 Material model

A linear elastic material model was used in this thesis to get a first understanding of how the crossmember behaves and since it simplifies the simulations. The usage of a linear material model under load cases that will cause plastic deformation will result in some implications. In points where yield stress is exceeded, the stress

will be overestimated. The steepness of the stress-strain curve usually decreases because of variation of stiffness in the structure and the variation of stiffness will not be captured in the material model used. Further, neglecting plastic deformations will lead to a structure that is stiffer than it actually is, a side effect is that the displacements in certain region can be underestimated.

5.3.2 Application of transient loads

Static loads was used to apply the crash loads on the crossmember. The static load does not change its magnitude or location over time which the crash loads does. A crash is a brief event with a transient load which varies in magnitude continuously. It can be established that there is a difference between the loads in the optimization and the actual crash loads but in an early design phase static loads gives a good indication on how the material should be distributed. It would be desirable to run a reanalysis of a realised geometry to further evaluate how well static loads work in an early design phase. Other transient load cases covered in the thesis are the road induced loads, which were also modeled as static loads in the BIW. Less thought was put into these loads as discussions with engineers at VCC lead to the conclusion that those loads did not have a large effect on the crossmember and how it was originally designed.

5.4 Conclusions

The most significant conclusions from this thesis is presented below.

- Trial cases showed that draw direction was a setting that should be used. The specific values of the sub-settings, such as minimum member size should be discussed with a manufacturing expert. The minimum member size is coupled with average element size.
- It is worth the effort to set-up a superelement to fully capture the behaviour of the BIW and to significantly reduce the computational time.
- It could be concluded that weight factors in the compliance index are a necessity if the load cases vary widely. Due to the complexity of choosing weight factors, some iteration is likely required.
- Topology optimization with linear and static crash loads can be used in early design to indicate where material is most needed, as well as where material is not needed.
- It is of importance to apply the crash loads as accurately as possible since their large magnitude will have a large impact on the rib structure.
- A design engineer who could create a CAD model of the best optimization is necessary to enable verification and more advanced simulations.

6

General guidelines

Based on the findings in the thesis, figure 6.1 on the next page shows the general guidelines for how to perform a topology optimization on an E-machine mount. To begin with, careful consideration must be taken when specifying the design space so that vital material is not removed. Perhaps the most challenging step when designing a new component which is part of a larger system is estimating the loads that will be exerted on it as the they will be dependent on multiple factors. Engineering estimations together with data from previous models will be a good first approximation when setting up the load cases.

The superelement is an important factor to capture the full behaviour of the BIW during crash scenarios. To both capture the behaviour of the surrounding components and reducing the computational time, as few ASETs as possible should be used without compromising the actual number of connections. To properly define the manufacturing constraint, experts within the area should be consulted in order the specify all parameters in a correct way. It is also of importance to use sufficiently small elements in the mesh, otherwise OptiStruct cannot fulfill the manufacturing constraints.

Lastly the objective functions and constraints are to be specified. The most common objective is to minimize the compliance. Compliance index has proved to be a good objective since it takes multiple load cases into consideration. If external loads are applied, the compliance should be minimized to maximize the stiffness of the crossmember. To reduce the volume, and effectively the mass, the volume fraction can be within a constrained interval.

After the optimization, the preliminary results should be reviewed and evaluated. If deemed good enough, the design should be realized and further evaluated. It was found in the thesis that certain engine load cases were neglected since the crash loads had significantly higher compliance. To compensate for the large difference in compliance, one can alter the weights in the compliance index and via that make specific load cases more or less important for the optimization algorithm and rerun the optimization.

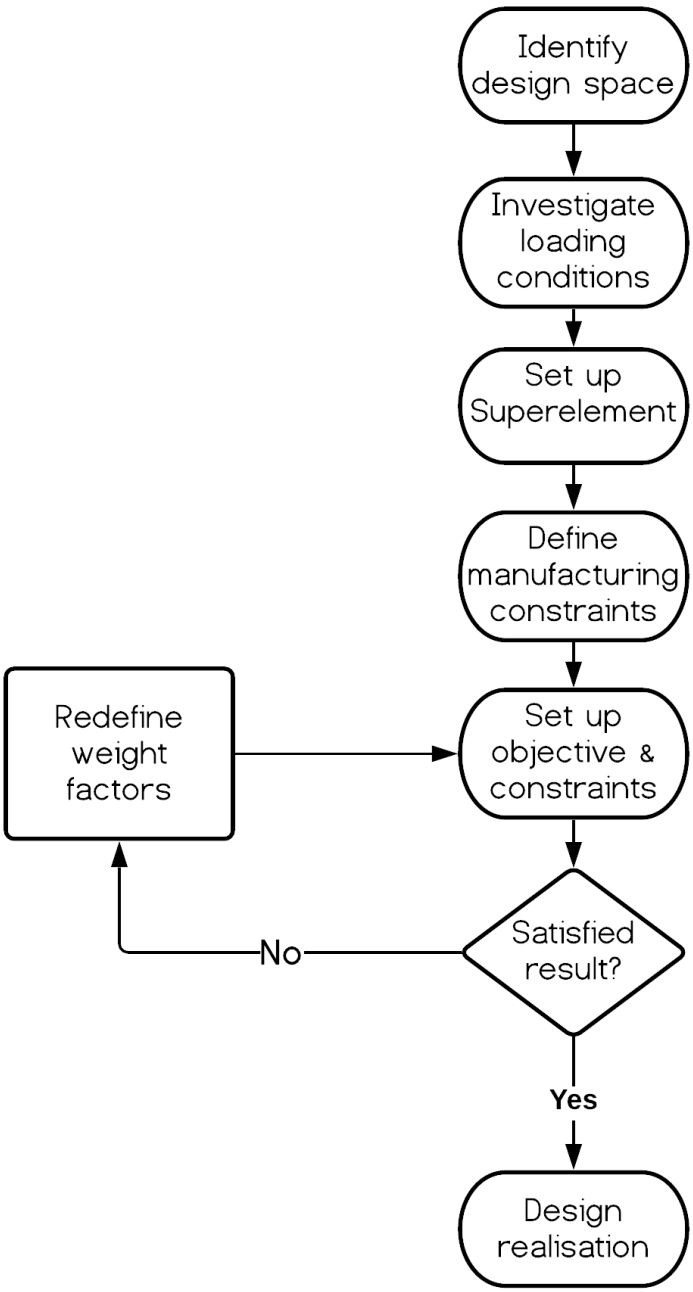

Figure 6.1: A flowchart of the recommended approach to set up a full topology optimization of an E-machine mount.

References

[Altair, 2021] Altair (2021). -Ver 2019.1. https://www.altair.com/optistruct/. Accessed: 2021-03-24.

[Andreassen et al., 2011] Andreassen, E., Clausen, A., Schevenels, M., Lazarov, B. S., and Sigmund, O. (2011). Efficient topology optimization in matlab using 88 lines of code. *Structural and Multidisciplinary Optimization*, 43(1):1–16.

[Bendsoe and Sigmund, 2013] Bendsoe, M. P. and Sigmund, O. (2013). *Topology optimization: theory, methods, and applications*. Springer Science & Business Media.

[Christensen and Klarbring, 2008] Christensen, P. W. and Klarbring, A. (2008). *An introduction to structural optimization*, volume 153. Springer Science & Business Media.

[OpenLearn, 2017] OpenLearn (2017). High pressure die casting. https://www.open.edu/openlearn/science-maths-technology/engineering-technology/manupedia/high-pressure-die-casting. Accessed: 2021-04-05.

[Siemens, 2014] Siemens (2014). Superelement User's Guide. https://docs.plm.automation.siemens.com/data_services/resources/nxnastran/10/help/en_US/tdocExt/pdf/super.pdf. Accessed: 2021-03-22.

A

Appendix 1

A.1 Rib structure for optimization with weight factors

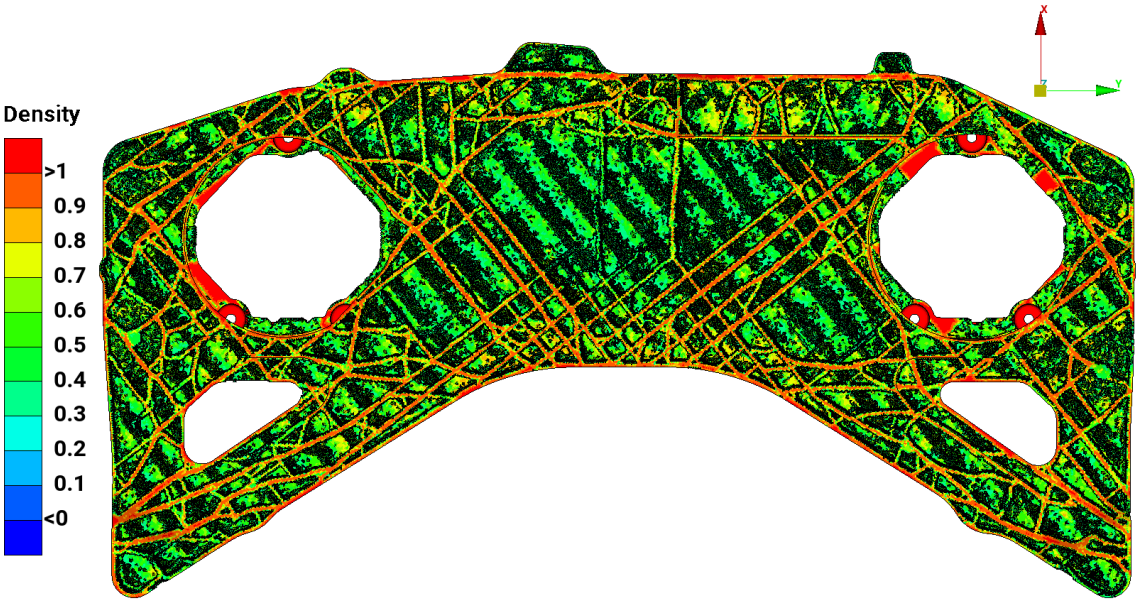

Figure A.1: Full rib structure with weighted load cases.

A.2 Contour plots of stresses on a divided crash load optimization

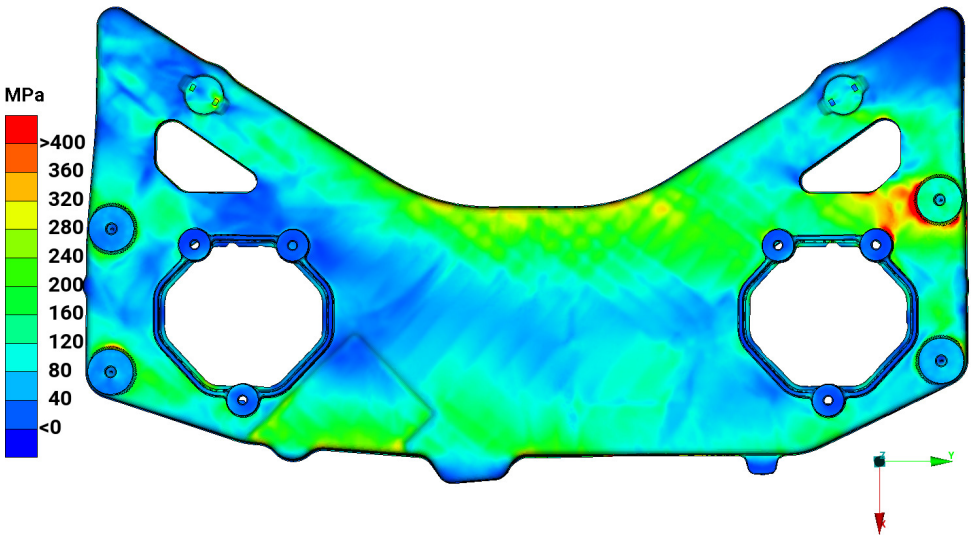

(a) Stress with a divided crash 1 load.

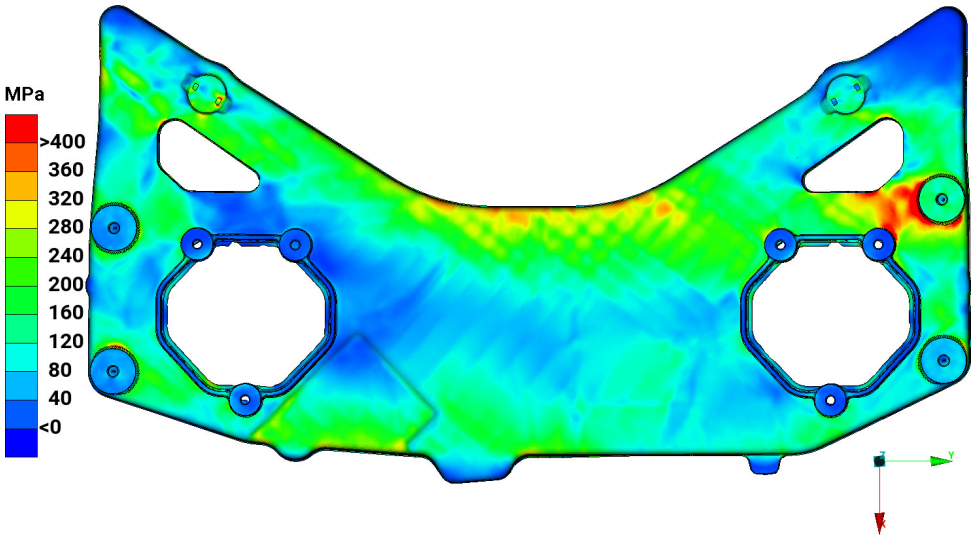

(b) Stress with a uniform crash 1 load.

Figure A.2: The stress distribution on the top side of the model optimized for a divided crash load.

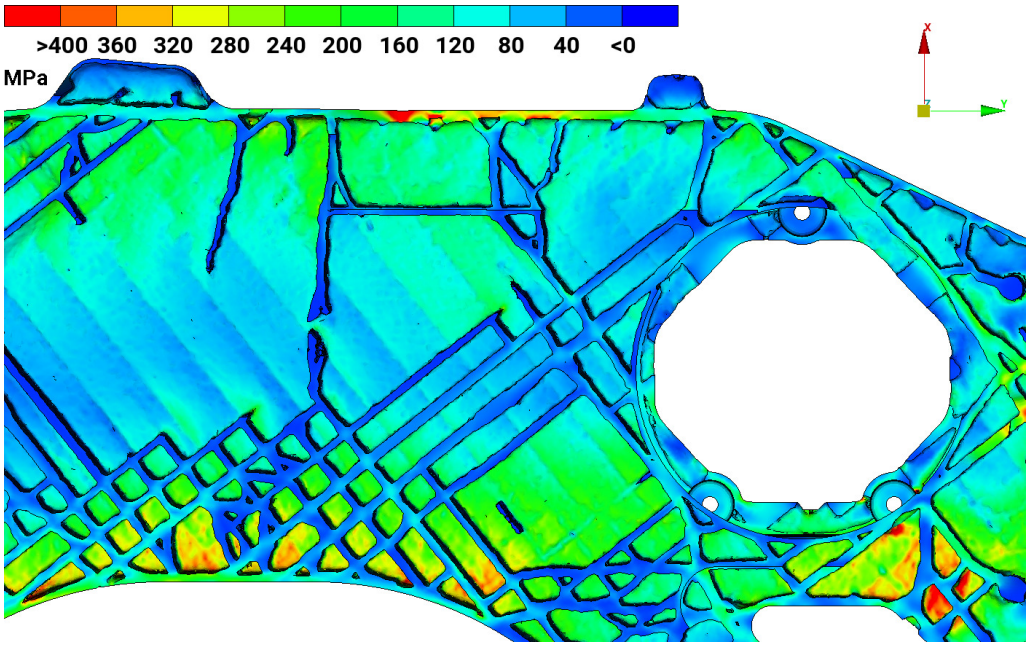

(a) Stress with a divided crash 1 load.

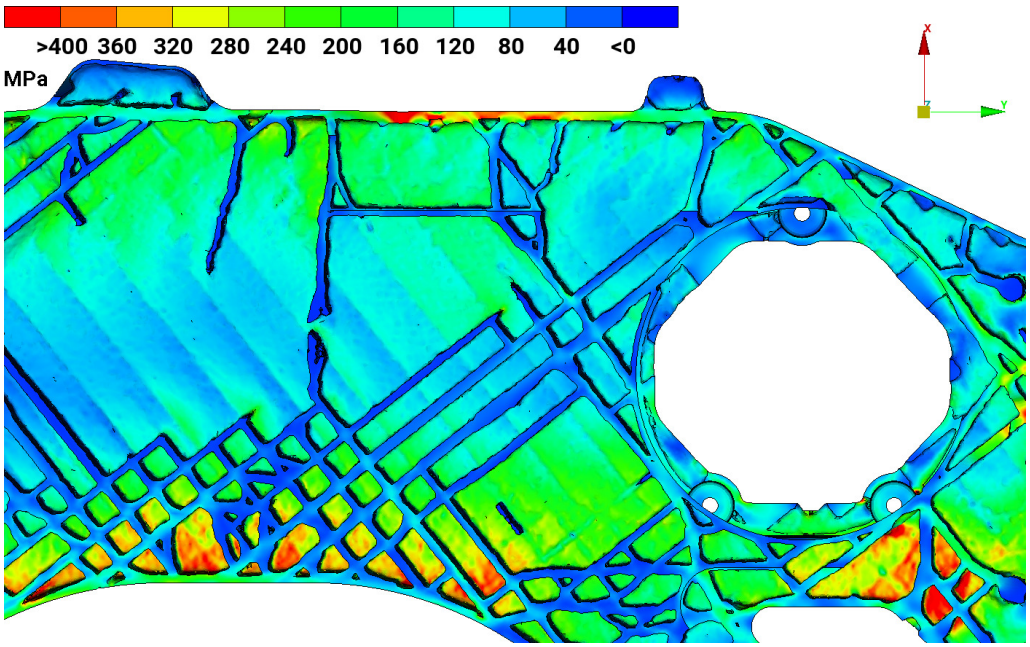

(b) Stress with a uniform crash 1 load.

Figure A.3: The stress distribution on the bottom side of the model optimized for a divided crash load. It can be seen that the stress is higher with a uniform crash load.

DEPARTMENT OF INDUSTRIAL AND MATERIALS SCIENCE
CHALMERS UNIVERSITY OF TECHNOLOGY
Gothenburg, Sweden
www.chalmers.se

CHALMERS
UNIVERSITY OF TECHNOLOGY